Ecological Modelling 498 (2024) 110863

Contents lists available at ScienceDirect

Ecological Modelling

journal homepage: www.elsevier.com/locate/ecolmodel

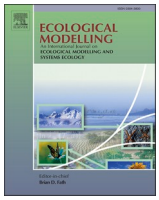

Spatial mechanistic modelling to simulate movements and contacts between wildlife and livestock in Southern Africa

Florent Rumiano [a,b,*], Eve Miguel [c,d], Victor Dufleit [b,e], Pascal Degenne [a,b], Cédric Gaucherel [f], Hugo Valls-Fox [g,h,i], Michel de Garine-Wichatitsky [j,k,l], Edson Gandiwa [m], Alexandre Caron [i,k,n], Annelise Tran [a,b]

[a] CIRAD, UMR TETIS F, 34398 Montpellier France
[b] TETIS, Univ Montpellier, AgroParisTech, CIRAD, CNRS, INRAE, 34090 Montpellier, France
[c] MIVEGEC, Univ. Montpellier, IRD, CNRS, 34090 Montpellier, France
[d] CREES Centre for Research on the Ecology and Evolution of DiseaSe–Montpellier, 34090 Montpellier, France
[e] CIRAD, UMR TETIS F- 97170 Petit-Bourg Guadeloupe France
[f] AMAP, IRD, CIRAD, CNRS, INRAE, Univ Montpellier, 34398 Montpellier, France
[g] CEFE, Univ Montpellier, CNRS, EPHE, IRD, Univ. Paul Valéry Montpellier 3, 34090 Montpellier, France
[h] LTSER France, Zone Atelier CNRS "Hwange", Hwange National Park, Bag 62 Dete, Zimbabwe
[i] SELMET, Univ Montpellier, CIRAD, INRAE, Institut Agro, 34090 Montpellier, France
[j] CIRAD, UMR ASTRE, F-34398 Montpellier, France
[k] ASTRE, Univ Montpellier, CIRAD, INRAE, 34090 Montpellier, France
[l] Faculty of Veterinary Medicine, Kasetsart University, 10900 Bangkok, Thailand
[m] Scientific Services, Zimbabwe Parks and Wildlife Management Authority, PO Box CY 140, Causeway, Harare, Zimbabwe
[n] Faculdade de Veterinaria, Universidade Eduardo Mondlane, 257 Maputo, Mozambique

ARTICLE INFO

Keywords:
African buffalo
Animal movement
Cattle
Mechanistic modelling
Remote sensing
Wildlife-livestock interface

ABSTRACT

The open interfaces between protected areas and rural communal lands in southern Africa are characterized by semi-arid savannas where wildlife-livestock interactions vary in frequency and intensity. In a context of increasing anthropization of land and trans-frontier conservation, the multiplication of these interactions may facilitate human-wildlife coexistence such as competition for natural resources, livestock predation, crop destruction by wildlife, and/or the risk of pathogen transmission between wild and domestic species. To better understand potential contacts between domestic and wild animals at these wildlife/livestock interfaces, we developed a method combining remote sensing and spatial modelling to simulate the movements of African buffalo (*Syncerus caffer*) and domestic cattle (*Bos taurus, Bos indicus*). Satellite-derived maps of surface water and vegetation, the primary determinants of movement for these ungulate species, were integrated into a mechanistic and stochastic model of collective movements of individuals interacting according to group cohesion and alignment. This model allowed simulations of herd movements and the location of contact areas with their seasonal dynamics in space and time at the periphery of three national parks in Zimbabwe and South Africa. Model outputs were compared to Global Positioning Systems collar location data of 32 individuals (14 buffalo and 18 cattle). The modelled results show a high spatial and seasonal variability of contacts between buffalo and cattle in the three study sites, and a landscape scale correspondence between spatial extensions of the modelled and observed contact areas. These results illustrate the potential of spatial modelling combined with remote sensing to generically simulate animal movements and contacts at landscape scale while providing opportunities to explore the management of these wildlife/livestock interfaces through, for example, a further coupling with epidemiological modelling.

* Corresponding author.
E-mail address: florent.rumiano@gmail.com (F. Rumiano).

https://doi.org/10.1016/j.ecolmodel.2024.110863
Received 8 March 2024; Received in revised form 2 September 2024; Accepted 3 September 2024
Available online 20 September 2024

1. Introduction

The increasing footprint of human societies and their extractive activities has heightened the demand for natural resources while causing the fragmentation of natural habitats (Hansen and Defries, 2007). Consequently, humans and their domestic animals are living in closer proximity to natural areas and wildlife (Wittemyer et al., 2008), thereby increasing the number of wildlife-livestock interfaces (WLIs). The establishment of Transfrontier Conservation Areas (TFCAs) in Southern Africa has further reinforced this trend by providing additional space for congested wildlife populations and extending their effective distribution range (Fynn and Bonyongo, 2011). WLIs, defined as the physical spaces where wild species, domestic species, and humans overlap in range and interact (Caron et al., 2021), include the movements of wild and domestic animals across the landscape (e.g., between communal land and protected areas) and determine potential direct and indirect contacts between species (Ferguson et al., 2012). WLIs within TFCAs are potentially subject to increasing human-wildlife encounters and interactions. The larger areas created to reduce human-wildlife conflict (HWC) can sometimes accelerate conflicts due to growing and expanding wildlife populations. From an anthropocentric perspective, HWC that pose threats to human agricultural activities and human life (Madden, 2004) include events such as livestock depredation by carnivores (Eklund et al., 2017), crop destruction by wildlife (Gross et al., 2018), increased competition for shared natural resources (Treves et al., 2006), hunting or illegal hunting (Warchol et al., 2003), and disease transmission (Decker et al., 2010). HWC can also be indirectly influenced by climatic events, which are becoming increasingly unpredictable in terms of frequency and intensity due to climate change (IPCC, 2023). These climatic events influence hunting strategies or cause stochastic environmental events (e.g., fire, flooding), which can drive animals towards anthropized areas (Distefano, 2005). Consequently, HWC fosters resentment from local communities, who may retaliate by killing wild animals, often illegally (Mbise, 2021). Given the complexity of human-wildlife conflicts locally, WLIs are at the epicenter of economic, social, health, and conservation issues (Frank et al., 2019). This complexity prompts stakeholders to design policy-relevant pathways toward human-wildlife coexistence (König et al., 2020) and coadaptation (Carter et al., 2020). In Southern African WLIs, livestock husbandry and subsistence agro-pastoralism are prevalent (Caron et al., 2013), impacting conservation within these multiple-use areas (Fynn et al., 2016). These WLIs are primarily located in semi-arid savannas, where the spatial distribution and availability of natural resources, such as forage and surface water, are influenced by seasonal variations and human activities, including agricultural expansion (Chagumaira et al., 2016). The spatiotemporal distribution of these resources, in turn, influences animal landscape use (G. Wang et al., 2006). During the dry season, forage and surface water become irreplaceable resources (Valls-Fox et al., 2018a), making their availability a key determinant of animal distribution at the landscape scale (Ogutu et al., 2014). In Southern African WLIs, competition for these natural resources can potentially lead to depletion effects, particularly when resources are concentrated in specific areas and periods (Chamaillé-Jammes et al., 2007; Shrader et al., 2008).

In this context, it is crucial to understand the drivers of resource selection by wild and domesticated animal species to mitigate HWC, including the risk of pathogen transmission (Miguel et al., 2013), by characterizing the spatiotemporal distribution of natural resources (Wiens, 1989), animal movement patterns (Gaucherel, 2011; Benhamou, 2014), as well as their respective foraging and watering decisions (Owen-Smith et al., 2010; Valls-Fox et al., 2018b). Spatial models that simulate collective animal movements at the landscape scale, accounting for biotic and abiotic drivers and including behavioral mechanisms, have recently been developed (Westley et al., 2018). The latest technological advances, such as the use of telemetry based on the global positioning system (GPS) (Kays and Crofoot, 2015) and the use of satellite remote sensing (SRS) (Remelgado et al., 2018), have led to major advances in the collection of data on animal movement and on their distinctive environments. This data, coupled with models of collective movements, provide a timely opportunity to better understand animal behaviors at high spatial and temporal resolutions. Previous studies used such models on other species and highlighted their benefits in explaining the collective behavior of animal groups (Sumpter, 2006; Giuggioli and Kenkre, 2014). Movement models applied at the individual and collective levels such as mixtures of random walks capturing the long-distance movements observed in many animals (Morales et al., 2004), state-space models analyzing movement data by estimating unobserved behavioral states and predicting future movements (Jonsen et al., 2005), Mechanistic Home Range models integrating movement behavior with spatially explicit resources to predict home range patterns (Sawyer et al., 2013) or agent-based models (ABMs) simulating the actions and interactions of individual animals to assess their effects on the system as a whole (Grimm et al., 2005), have all helped to enhance our capabilities to better understand and predict animal behavior and interactions. The collective movement model developed in this article is based on a self-propelled collective motion model developed by (Grégoire et al., 2003) and differs from previous animal movement models as it focuses on the collective and cohesive motion in animal groups, distinguishing it by its specific attention to the forces of cohesion and alignment among individuals. Developing such a model designed to simulate movements influenced by interactions with other individuals and the environment could potentially provide a more detailed and dynamic understanding of group movement behaviors of buffalo and cattle in different ecological and environmental contexts. However, the development of collective movement models comes with challenges such as the integration of habitat heterogeneity and individual-level variations into analyses of collective movement, as well as the computational power required to process large amounts of data (Westley et al., 2018).

The African buffalo (*Syncerus caffer*) and domestic cattle (*Bos taurus, Bos indicus)* are both large bovid species and key players in conservation and production systems in Southern Africa. As primarily grazing animals of similar size, they depend on and compete for the same natural resources when they are sympatric (Kock et al., 2023; Fynn et al., 2016; Odadi et al., 2011). We posit that a better understanding of the movement dynamics of these two species in time and space can provide insights into ecological phenomena, such as inter-species relationships (Rumiano et al., 2020). Enhancing our comprehension of these relationships may help address and mitigate the rising risk of disease transmission between these species and potentially to humans (Miguel et al., 2013). From that standpoint, this study aims to develop a spatial mechanistic model to simulate buffalo and cattle movements based on seasonal surface water availability (Caron et al., 2023a; Rumiano et al., 2021) and their respective interactions with the landcover according to their inherent behaviors. The primary objective of the model is to assess the frequency and geographical location of buffalo-cattle contacts at a medium spatial scale in three WLIs areas near protected areas in Zimbabwe and South Africa.

2. Method

2.1. Study sites

The three study sites (Fig. 1) are located on the periphery of protected areas: i) in Zimbabwe, Hwange National Park (HNP), referred to as “Hwange/Dete”; ii) Gonarezhou National Park (GNP), referred to as “Gonarezhou/Malipati”; iii) and in South Africa, Kruger National Park (KNP), referred to as “Kruger/Pesvi” with a periphery in Zimbabwe. The “Hwange/Dete” study site, located west of Zimbabwe close to Botswana and Zambia, is approximately 600 km from the two other study sites in a straight line. On the other hand, the “Gonarezhou/Malipati” and “Kruger/Pesvi” study sites, located southeast of Zimbabwe near

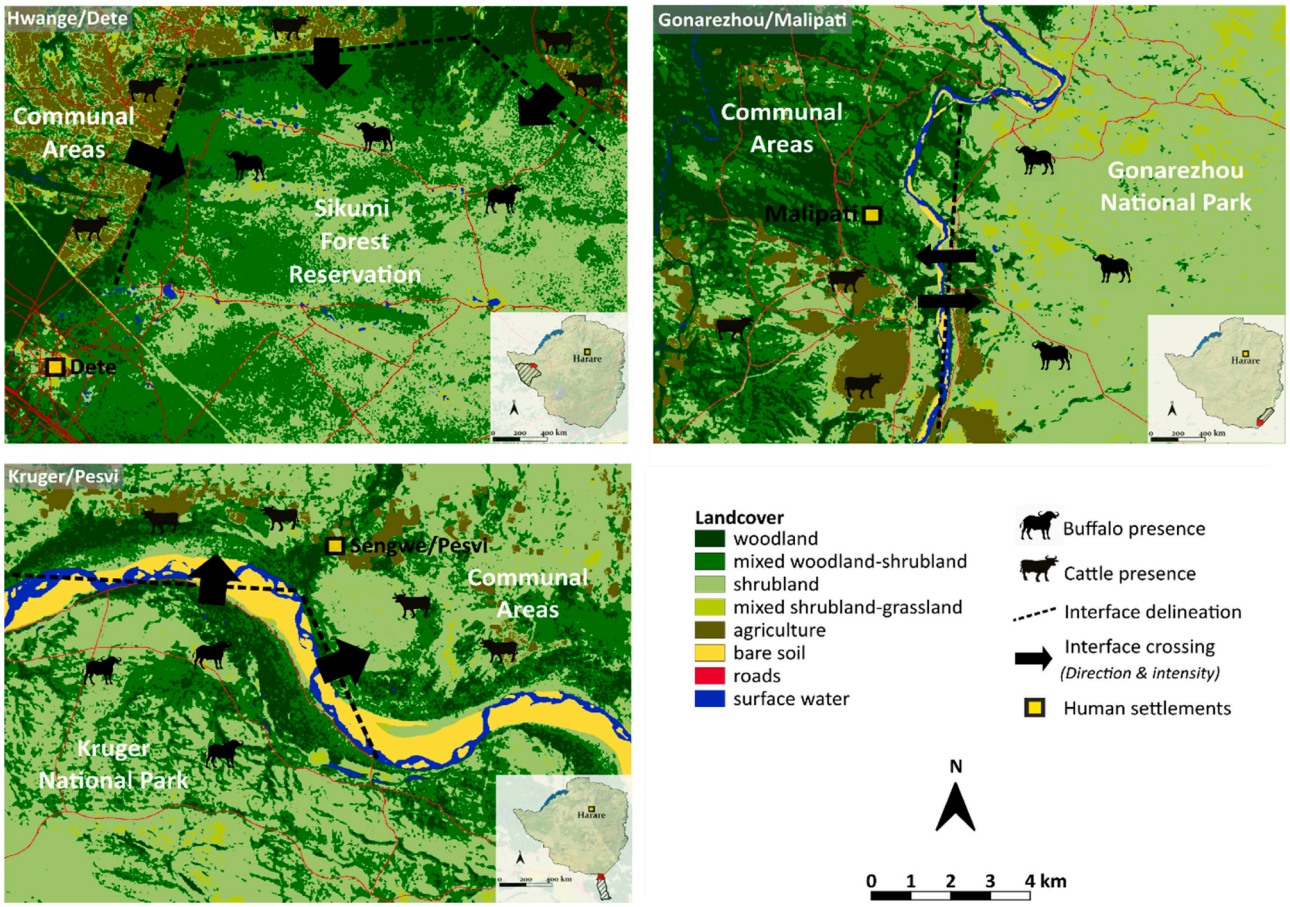

Fig. 1. Location maps of the three study sites. Note that the interface delineations are not based on administrative borders. Their shapes and locations serve as illustration purposes and translate ecological assessments realized in-situ.

Mozambique and South Africa, are just approximately 50 km apart in a straight line. In these three sites, conflicts between human communities and wildlife are increasing (Mutanga et al., 2017; Guerbois et al., 2012), and boundaries between protected areas and communal areas are often permeable (i.e., river, railroad, or road) and without barriers.

In the three study sites, human activities in communal areas outside national parks primarily consist of subsistence farming with small-scale livestock production and rainfed agriculture (from November to March). Small herds are bred extensively with an average of 12 heads of cattle and small ruminants (goats and a few sheep) per herder (Miguel et al., 2013). In these areas, domestic and wild animal movements between natural and anthropogenic compartments are frequently observed in both directions (Chigwenhese et al., 2016), and contacts between African buffalo and domesticated cattle have been noted (Miguel et al., 2013), even though livestock incursions into protected areas are strictly forbidden in Zimbabwe and South Africa (Chigonda, 2018). The intensity and frequency of contacts vary among the study sites, emphasizing different buffalo and cattle contact configurations (Fig. 1). Based on the statistical analyses developed in a previous study (Miguel, 2012), the rate of cattle incursion inside protected areas (expressed as a percentage of the overall time recorded by the GPS collars placed on targeted cattle) was 6.9 % in Hwange/Dete, 3 % in Gonarezhou/Malipati, and 0.2 % in Kruger/Pesvi. Concerning the rates of buffalo incursion into communal areas, it was 0.05 % in Hwange/Dete, 7.46 % in Gonarezhou/Malipati, and 58 % in Kruger/Pesvi.

The three study sites are located in semi-arid climates with annual mean temperatures of 22 °C and mean annual precipitation ranging from 450 to 650 mm for Hwange/Dete (Chamaillé-Jammes et al., 2007), and mean annual temperatures ranging from 25 °C to 27 °C and mean annual precipitation ranging from 300 to 600 mm in both Gonarezhou/Malipati and Kruger/Pesvi. On average, excluding climatic anomalies (e.g., drought), the dry season occurs from April-May to October-November and the wet season from November to March for the three study sites. The vegetation in these areas is typical of a highly heterogeneous dystrophic wooded savanna (Arraut et al., 2018). The woody cover increases with distance from water pans (Chamaillé-Jammes et al., 2009), and the open grassland is located along drainage lines. In Hwange/Dete, the surface water mainly consists of seasonal natural pans of different sizes widely distributed across the area, complemented with artificial pans fed by underground water pumping stations during the drier months. In Gonarezhou/Malipati and Kruger/Pesvi, the surface water is composed of river systems with water along their entire courses during the wet season. During the dry season, intermittent river branches inside the riverbed and ephemeral rainfed natural pans located on sandstones are present and constitute primary water resources for wild and domestic animal species alike.

2.2. Telemetry data

Collars manufactured by African Wildlife Tracking have been used in previous studies to monitor the movements and contacts between selected cattle and buffalo herds (Miguel, 2012; Valls Fox, 2015). The collars were equipped with Iridium Satellite Tag (Iridium Satellite and Ultra-High Frequency - UHF) providing secure near real-time GPS animal tracking with meter accuracy. UHF, referring to the portion of the radio frequency spectrum from 300 MHz to 3 GHz presents several advantages in the animal tracking data context. UHF have been chosen because of its favorable propagation characteristics such as range and

penetration (UHF signals have a shorter range compared to lower frequency bands like VHF but offer better penetration through a wide variety of terrain) as well as extended coverage (communications can be maintained even in remote and challenging environments as the UHF system consists of 66 active satellites in low Earth orbit).

The UHF telemetry data were collected at different periods of time (Appendix A) but with the same time frequency (i.e., 1-hour) at the three study sites. In total, 10 cattle and 8 buffalo individuals were monitored in Hwange/Dete, 4 cattle and 2 buffalo individuals in Kruger/Pesvi, and 4 cattle and 4 buffalo individuals in Gonarezhou/Malipati (Appendix A). The data have been pre-processed to derive metrics allowing the design and validation of the movement model used in this study. Pre-processing steps included: 1) The re-projection of the entire telemetry dataset, the correction of outlier data, and the harmonization of time delays, all following the methodology developed by Wielgus (2020a); 2) The grouping of buffalo and cattle telemetry data by locations and time of recording for each of the three study sites to derive herd entities sharing the same location at the same time.

2.3. Pre-processing of remote sensing data

Seventy-two Sentinel-2 satellite images (Drusch et al., 2012) acquired in 2018 and covering the three study sites have been downloaded in Level 1C, which provides Top of Atmosphere reflectance and orthorectified images (Appendix B). The Sen2Cor v2.8 application (Sen2Cor, ESA, http://step.esa.int/main/third-party-plugins-2/sen2cor/) has been used to apply atmospheric corrections, thus transforming L1C images to Level L2A (Top of Canopy) images. Six tiles were required to cover the entire spatial extent of the three study sites. The dates of the selected images represent days with <10 % cloud cover for the entire year 2018, with one image per month for each tile. For the month of February, however, no images were cloud-free in 2018. As a result, Sentinel-2 satellite images from February 2019 have been selected instead. The 20-meter spatial resolution spectral bands of the L2A Sentinel-2 images have been resampled by bilinear interpolation to 10-meter spatial resolution while ensuring the continuity of the WGS84/UTM35S and WGS84/UTM36S projection systems and clipped to correspond to the respective spatial extent of the three study sites. Sentinel-2 satellite images were selected due to their higher spatial resolution and detailed spectral bands, which offer more precise information for surface water and landcover classification compared to older data, such as Landsat satellite images. Although there is a temporal offset between the Sentinel-2 images and the telemetry data used in this study (refer to the "Telemetry Data" section), the year 2018 was specifically chosen because it accurately reflects the current environmental conditions observed in situ during fieldwork. Furthermore, advanced processing techniques optimized for Sentinel-2 data enable more precise analysis, enhancing the study's relevance and alignment with contemporary research efforts regarding surface water and landcover classification (Du et al., 2016).

2.4. Surface water and landcover detection

The detection of surface water and landcover is designed in three steps (Fig. 2) that correspond respectively to surface water classification (Step 1), agricultural area classification (Step 2), and vegetation

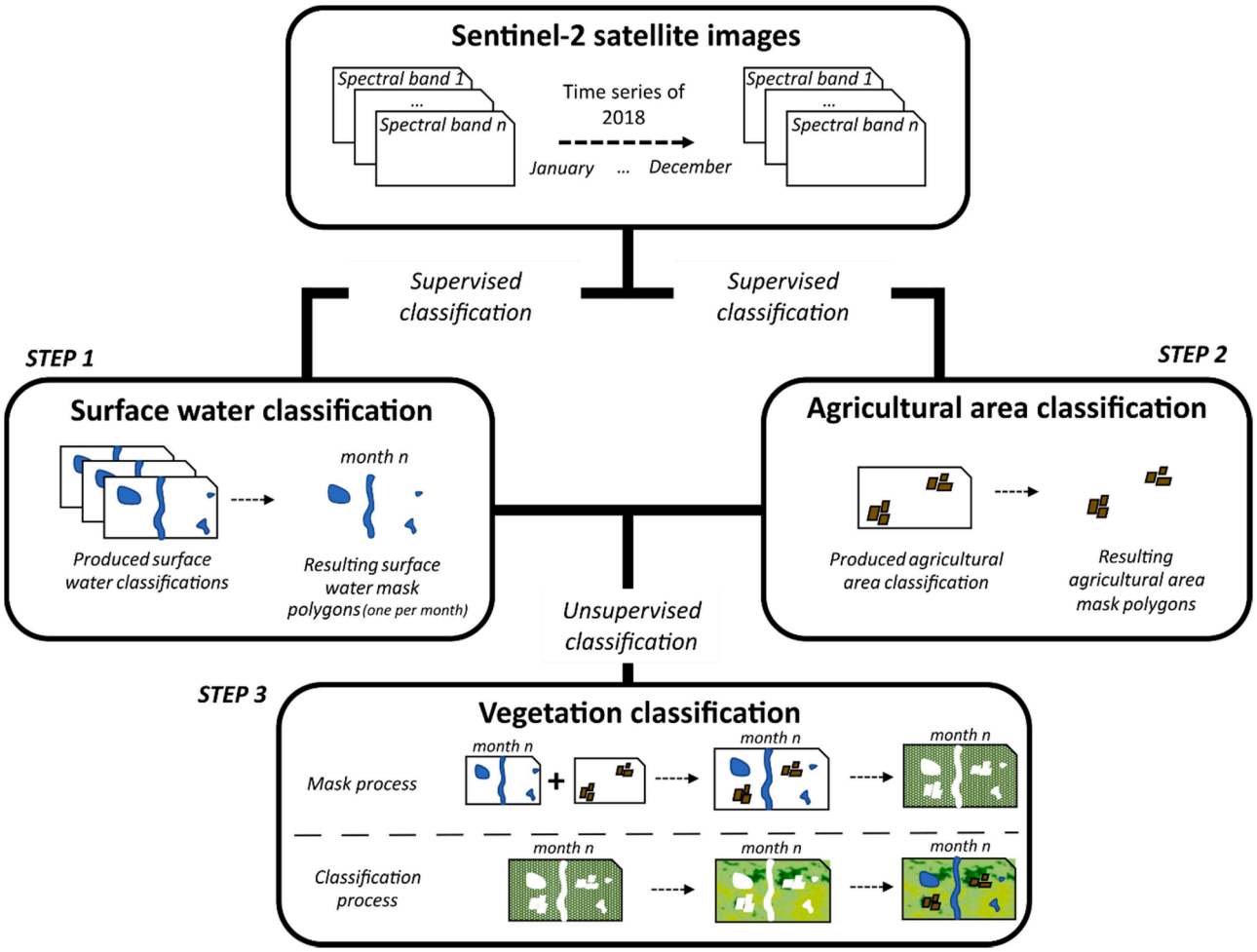

Fig. 2. Classification general process in three main steps: 1) surface water classification, 2) agricultural area classification, 3) vegetation classification.

classification (Step 3).

Surface water classification: Two water indices, the Modified Normalized Difference Water Index (MNDWI) and the Normalized Difference Water Index (NDWI), were computed from Sentinel-2 images following Du et al. (2016). A set of 100 reference polygons (tagged as "surface water" or "other") were delineated from image interpretation using very-high spatial resolution SRS images (e.g., Airbus provided Pleiades satellite images of 50 cm spatial resolution) accessed via the XYZ Tile tool in the QGIS software (version 3.35.1 "Prizren") and split into a 50/50 ratio to constitute a reliable comparison between training and validation samples (Mercier et al., 2019). The classification using the Random Forest (RF) algorithm was then applied using the methodology developed in Rumiano et al. (2021). The algorithm produced a time series of classified rasters at a spatial resolution of 10 m for each of the study sites. All rasters were then converted to vector layers to facilitate subsequent processing steps. The vector layers for March, representing maximum water extents due to peak precipitation, were selected as templates for each tile. Subsequently, these March vector layers were used to mask noise polygons from the vector layers of the other 11 months across all three study sites.

Agricultural areas classification: Vegetation indices, namely the Normalized Difference Vegetation Index (NDVI), the Enhanced Vegetation Index (EVI), and the Soil Adjusted Vegetation Index (OSAVI) (Fern et al., 2018), were derived from Sentinel-2 images for the month of March, corresponding to the peak of the wet season when the contrast between vegetation and bare soil is strongest. These spectral indices were considered for supervised classification of agricultural areas, as they have proven efficient in previous studies for characterizing such areas using medium spatial resolution SRS images (Bellón et al., 2017; Y. Zhao et al., 2020). A set of 100 reference polygons (tagged as "agricultural areas" or "other") were delineated from image interpretation using very-high spatial resolution SRS images (e.g., Airbus provided Pleiades satellite images of 50 cm spatial resolution) accessed via the XYZ Tile tool in the QGIS software (version 3.35.1 "Prizren") and were split into a 50/50 ratio. Supervised classifications were then performed using the RF algorithm. The resulting classification rasters were subsequently vectorized to manually detect and remove false positives.

Vegetation classification: Three Sentinel-2 red-edge spectral bands (band 5, band 6, and band 7) were masked using manually digitized polygons of road networks, surface water, and agricultural areas. These masked bands were then utilized to classify five vegetation and landscape classes (woodland, mixed-woodland shrubland, shrubland, mixed shrubland-grassland, bare soil) at each of the three study sites. The classification employed a pixel-based non-supervised K-means clustering method (Burrough, van Gaans, and MacMillan, 2000). Previous studies have shown that the inclusion of red-edge bands in the classification scheme improves the characterization of vegetation classes and overall classification accuracies (Schuster et al., 2012).

Post-classification: For each of the study sites, the rasters produced from the non-supervised classification were combined with its respective surface water, agricultural area, and road network rasters to create final landcover classification rasters of an eight-element typology (Fig. 1) at a spatial resolution of 10 m.

Classification validation: Regarding the surface water and agricultural areas classifications (steps 1 and 2), sets of reference polygons from the three study sites were used as training and validation data to perform cross-validation using two classification accuracy indicators: overall accuracy (OA) and Kappa index. Fifty iterations of classification were conducted using randomly selected reference polygons for each study site to assess the robustness and stability of the classification method. For the validation of the non-supervised classification of vegetation (step 3), three sets of reference polygons (one for each study site) were manually digitized "a priori" before classification. These polygons consisted of 50 reference polygons per class and were derived from photo-interpretation using very-high spatial resolution SRS images (e.g., Airbus provided Pleiades satellite images of 50 cm spatial resolution) accessed via the XYZ Tile tool in the QGIS software (version 3.35.1 "Prizren") for each study site. The reference polygon datasets were then used to calculate the OA and Kappa index for the vegetation classifications.

2.5. A spatialized movement model

A model of collective motion of self-propelled individuals (Grégoire et al., 2003)has been chosen to model the two focal species movements at the individual and herd scales as developed in Rumiano et al. 2021 (1). In this model, each individual i moves from its starting location to the next at discrete time steps by a fixed distance v_0, its direction defined for each timestep t as an angle θ_i^t:

$$\theta_i^{t+1} = \arg\left[\alpha \sum_{j \neq i} \vec{v}_j^{\,t} + \beta \sum_{j \neq i} \vec{f}_{ij}\right] + h\xi_i^t \quad (1)$$

α (1) regulates the *herd alignment* (expressed as the sum of all other individuals' speed vectors $\vec{v_j}$) and may vary according to herd behaviour (Table 1): when α is null, the model simulates a situation where the herd remains stationary (such as during a rumination phase) whereas when $\alpha \neq 0$, the model simulates a movement of the herd with a direction (for example during the phase when the animals are moving towards a surface water); β (1) regulates the *herd cohesion* (expressed as the sum of the vectors $\vec{f_{ij}}$ that link two individuals i and j) and is fixed; However, $\vec{f}_{ij}$ is regulated by repulsion and attraction forces between individuals and is expressed as follows:

$$\vec{f}_{ij} = \vec{e}_{ij} \begin{cases} -\infty \ if \ r_{ij} < r_{c,} \\ \frac{1}{4} \frac{r_{ij} - r_e}{r_a - r_e} \ if \ r_c < r_{ij} < r_a \\ 1 \ if \ r_a < r_{ij} < r_0 \end{cases} \quad (2)$$

$\vec{f}_{ij}$ (2) is characterized by several sub-parameters—namely, the limit of interaction distance, the repulsion distance, the equilibrium distance, and the minimal distance (Table 1). These sub-parameters define the intrinsic ecological cohesion behavior of individuals within a collective, thereby establishing species distinctiveness within the model's conceptual framework. The limit of interaction distance (r_0) represents the maximum distance within which an individual can interact with other individuals. Any individuals beyond this distance are not considered when calculating the forces (i.e., attraction/repulsion) acting on a given individual. This distance sets the spatial scale of the interaction neighborhood. The repulsion distance (r_c) is the distance below which two individuals start to experience a strong repulsive force. The purpose of this force is to prevent the individuals from overlapping or getting too close to each other. This distance helps to maintain a minimum

Table 1
Model parameters estimated from telemetry data (*), expert knowledge (**), or calibration (***) (for the estimation of the animal speed, see details in the Appendix C, for the calibration of alpha, beta and the noise, see details in (Rumiano et al. 2021)).

Parameters	Definition	Values Buffalo	Values Cattle
v_0	animal speed	0.24 km/h*	0.46 km/h*
r_0	limit of interaction distance	500m**	300m**
r_c	repulsion distance	5m**	0.5m**
r_e	equilibrium distance	10m**	5m**
r_a	minimal distance	150m**	150m**
α_0	alignment regulation – resting or rumination/drinking phases	0.0**	
α_1	alignment regulation - randomly move	1.2***	
α_2	alignment regulation – directional move	1.6***	
β	cohesion regulation	1***	
h	noise regulation	0.4***	

separation between individuals, avoiding physical collisions. The equilibrium distance (r_e) corresponds to the distance at which the attractive and repulsive forces between individuals balance each other out, resulting in no net force. At this distance, individuals are neither pushed away nor pulled towards each other. It can be thought of as the optimal spacing where the herd is in a state of equilibrium. The minimal distance (r_a) is the shortest distance observed between any two individuals. It can be influenced by the repulsion distance, as individuals should ideally not come closer than this specified distance due to the repulsive forces in play. This distance helps in quantifying the closest approach between individuals. For buffalo and cattle, the values of these sub-parameters are based on empirical knowledge and in-situ observations (Table 1).

In addition to the parameters α (1) and β (1), h (1) represents deviations (i.e., noise) from the deterministic part of the model, which includes the forces (i.e., attraction, repulsion, alignment and cohesion) with which the direction of each individual is influenced by the others (ξ being a random angle). A higher noise value means more significant deviations, leading to more erratic movement, while a lower noise value means less deviation and more orderly movement. The value h (1) is fixed. For more detailed information regarding (1) and (2), please refer to Rumiano et al. 2021.

2.6. Application: designing a buffalo - cattle contact model

The movement model is applied to simulate the respective movements of the two focal animal species, the African buffalo and domestic cattle, aiming at determining the geographical location, frequency and temporality of their contacts at the three studied WLIs. For each species, the model simulates their respective movements over a 24-hour period, considering their main behavior phases, i.e., feeding, drinking and resting (Fig. 3).

Behavior phases: During the first "feeding phase," which occurs at night from 9pm to 7am, the buffalo herd moves until it reaches suitable landcover. Subsequently, it enters a "ruminating phase" before moving towards a surface water point during the "drinking/feeding phase." Upon reaching the designated surface water point, the herd remains nearby to drink before randomly dispersing across the landscape, thus completing the 24-hour period. In contrast, cattle behavior varies significantly due to domestication, where human decisions directly influence their movements in both space and time. A cattle herd typically spends most of its time within the confines of its enclosure or "kraals," serving as a central place. Outside the kraal, the herd grazes while moving across the landscape. When it's time to drink, the herd heads towards a surface water point where it can also feed, before returning to its enclosure for protection from predators at night. Throughout these behavioral phases, the movements of both buffalo and cattle are simulated according to Eq (1), with different values of α, which determines herd alignment (see Table 1) (Fig. 3).

Impact of the landscape: Surface water availability and landcover types, derived from Sentinel-2 images (as described in the previous section), are critical factors influencing the mobility of buffalo and cattle in the model. Each species follows specific rules for selecting feeding and watering areas during different behavior phases.

For buffalo, during the 'feeding phase,' a patch of suitable landcover (such as mixed-woodland-shrubland, shrubland, mixed shrubland-grassland) is chosen within a buffer. The buffer's radius corresponds

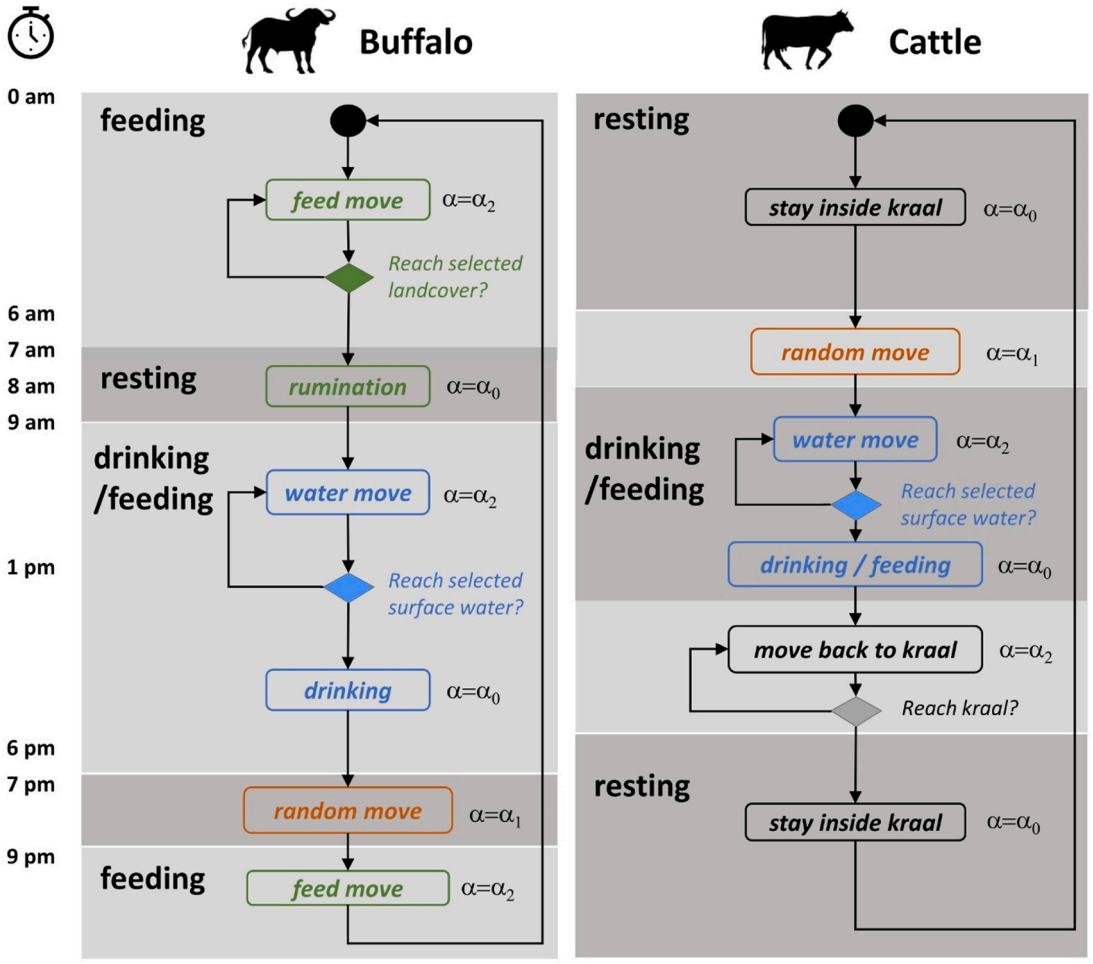

Fig. 3. Diagram representing the designed behavioral chronologies of the two focal species movement models (the buffalo model and the cattle model).

to the average distance traveled per hour by buffalo individuals. In the subsequent 'drinking/feeding' phase, the buffalo herd selects the nearest available surface water point based on their centroid position. It's important to note that the availability of surface water varies seasonally and is depicted using monthly surface water maps derived from Sentinel-2 images.

In contrast, cattle movements are influenced by herder decisions, solely with regard to the seasonal avoidance of crops. During the cropping season (December to April in Hwange/Dete, November to April in Kruger/Pesvi, and January to June in Gonarezhou/Malipati), cattle are directed away from cultivated fields to prevent crop damage. Outside of this period, they are allowed to move freely in agricultural areas to feed on secondary agricultural products (Miguel, 2012; Perrotton et al., 2017). During the 'drinking/feeding' phase, the suitability of surface water points is evaluated based on a 'suitability' score. This score considers both proximity to the cattle herd's centroid and the proportion of suitable landcover within a 50-meter buffer. Thus, water selection for cattle is influenced by seasonal cropping activities, where crop areas are deemed 'unsuitable' during the cropping season.

2.7. Choice of the modelling language

The modelling approach utilizes the domain-specific language Ocelet (Degenne and Lo Seen, 2016) to implement the buffalo-cattle contact model. Ocelet, integrated with a modelling platform (www.ocelet.org), specializes in spatially explicit modelling of dynamic systems. It facilitates the incorporation of geographic information, such as vegetation and water surface maps. In the Ocelet formalism, the buffalo-cattle contact model encompasses six interacting spatial entities: (i) buffalo individuals, (ii) buffalo herd, (iii) cattle individuals, (iv) cattle herd, (v) surface water, and (vi) landcover. A simulation is defined as a 'scenario' where these entities evolve over time, interacting with each other dynamically (e.g., interactions between buffalo individuals and buffalo herd, buffalo herd and surface water, etc.).

2.8. Simulations

Buffalo individuals present at the same time and in the same area with inter-distances inferior to one kilometer were considered to form observed groups (i.e., buffalo herds). As a result, considering the entire telemetry dataset, seven buffalo groups, each with different numbers of individuals, have been constituted across the three WLIs (two buffalo groups for Gonarezhou/Malipati, three buffalo groups for Hwange/Dete, and one buffalo group for Kruger/Pesvi). The grouping of individuals therefore dictated the considered time periods for the simulations. In total, seven simulation time periods, each corresponding to a constituted buffalo group, were computed (Appendix A). All buffalo group's simulation time periods had a one-hour time frequency (i.e., time step) to match the time frequency of the buffalo telemetry dataset. The lasting of the simulation time periods differs between constituted groups and can range from 133 days to 871 days, depending on the buffalo telemetry data recording time periods (Appendix A). For every simulation, one herd consisting of 200 buffalo individuals was modeled to correspond to the order of magnitude of buffalo herd sizes observed at the three study sites in previous studies (Miguel et al., 2013; Valls-Fox et al., 2018a). For each buffalo simulation, the starting point corresponds to the centroid location of each constituted groups at the earliest date (i.e., hour:day:month:year) of the corresponding telemetry data.

Similarly, for cattle, simulated herds were created with a random number of individuals ranging from 5 to 15, reflecting field observations (Miguel, 2012). Each simulated herd were to represent individual cattle at time periods corresponding to the observed cattle data considering that none of the collared cattle constituting the telemetry dataset were part of the same herd nor being linked to the same enclosure. Taking the entire telemetry dataset into account, eighteen cattle groups have therefore been modeled with their respective simulation time periods being synchronized with the recording periods of the observed cattle individuals for each study site (Appendix A - 4 periods for Gonarezhou/Malipati, 10 periods for Hwange/Dete, and 4 periods for Kruger/Pesvi). All cattle group's simulation time periods had a one-hour time frequency (i.e., time step) to match the time frequency of the cattle telemetry dataset. The lasting of the simulation time periods differs between constituted individuals (with the exception of three time periods concerning eleven individuals) and can range from 243 days to 735 days, depending on the cattle telemetry data recording time periods (Appendix A). The starting point of the simulation corresponds to the enclosure location attached to a specific collared individual from the telemetry dataset with the earliest date (i.e., hour:day:month:year) considered as the initial time.

All the buffalo and cattle simulation time periods have been synchronized with telemetry data where buffalo and cattle individuals have overlapping recording time periods (Appendix A). In addition, for every buffalo and cattle constituted groups, 10 simulation iterations have been computed to express and measure the stochasticity nature of the model.

2.9. Comparison with observed data

To compare observed and simulated datasets, we calculated the centroids of four randomly selected buffalo individuals within simulated herds (comprising 200 individuals), the centroids of in-situ buffalo groups (ranging from two to seven individuals), and the centroids of simulated cattle herds (ranging from 5 to 15 individuals) at hourly intervals. Centroids were computed using the "Centroids" tool in QGIS software (version 3.35.1 "Prizren"), located in the "Processing Toolbox" under "Vector Geometry Tools." Each centroid represents the central point for simulated buffalo, observed buffalo, and simulated cattle at time T.

To represent the space use and contact areas of observed and simulated buffalo and cattle, Kernel Density Estimations (KDEs) were calculated from centroid datasets for each of the three WLIs, across all simulation periods, as well as on a monthly basis. Intersection areas between KDEs derived from observed centroid datasets and KDEs derived from simulated centroid datasets for corresponding time periods were also computed. For each simulation, we performed 10 iterations and used the maximum spatial extent KDE (KDE-max) and the minimum spatial extent KDE (KDE-min) from these iterations to derive intersection areas with the observed KDEs for the corresponding time periods. We focused on 95 % KDEs to emphasize core areas of buffalo and cattle activity, reducing the influence of atypical movements, potential location errors, and infrequent long-distance excursions. The 95 % KDEs provide a statistically robust and ecologically relevant estimate by excluding the extreme 5 % of location data, which often consists of outliers or occasional exploratory movements not representative of the animals' regular home range (Silverman, 1998; Börger et al., 2006). KDE also offers a standardized method for comparisons across areas and species, facilitating meta-analyses and comparative studies (Worton, 1989; Laver and Kelly, 2008). Univariate KDEs were computed using the "ks" package version 1.14.2 (Duong, 2021) in R programming language (R version 4.4.0). The optimal bandwidth selection (i.e., smoothness of the kernel density estimate) was set to 2 stages, with a Smoothed Asymptotic Mean Squared Error (SAMSE) pilot bandwidth, and data pre-transformation using "sphere" normalization to ensure scale-invariance. Fig.4 illustrates the herd centroids and their corresponding annual KDEs for simulated and observed buffalo centroid datasets.

Additionally, we computed an index of buffalo-cattle contact rate using the method outlined by Miguel et al. (2013). We defined a potentially infective contact for foot-and-mouth disease as occurring when a cattle location was recorded within 500 m of a buffalo location within a 15-day temporal window. These parameters were selected to account for the potential survival of the pathogen in the environment and the precision of herd centroid locations. The number of contacts

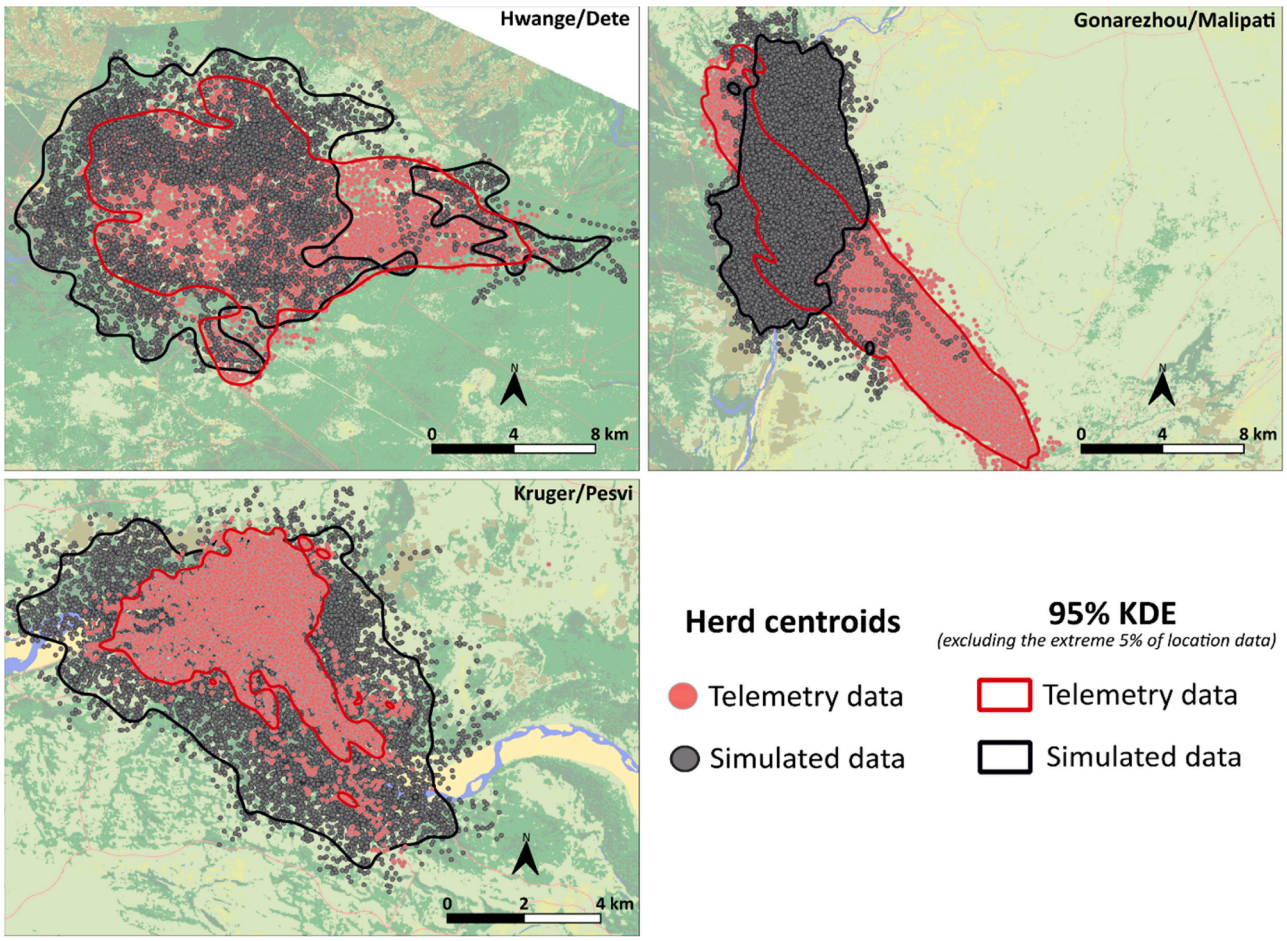

Fig. 4. Illustration of observed and simulated centroids of one buffalo herd and corresponding Kernel Density Estimations (KDEs) in Hwange/Dete, Kruger/Pesvi and Gonarezhou/Malipati Wildlife-Livestock-Interfaces.

meeting this criterion was divided by the total number of cattle herd locations and buffalo herd locations recorded within the same study site. To standardize the contact rate estimates, they were scaled by 108 and then logarithmically transformed, in accordance with Miguel et al. (2013). The buffalo-cattle contact rate indices were computed from both simulated and observed centroid datasets for buffalo and cattle on a monthly basis.

3. Results

3.1. Environmental variables characterized at a landscape scale

The supervised surface water classification demonstrates notably high accuracy across the three study sites. In Hwange/Dete, the mean overall accuracy (OA) of the time series supervised classification is 0.88, with a kappa index of 0.75. Comparatively, Gonarezhou/Malipati achieves an OA of 0.99 and a kappa of 0.97, while Kruger/Pesvi shows an OA of 0.97 and a kappa of 0.93. However, the supervised classification in Hwange/Dete slightly underperforms relative to the other sites, with accuracy ranging from OA 0.81 to 0.91 and kappa 0.63 to 0.82 within its time series. In contrast, classification accuracy remains stable throughout the time series for Gonarezhou/Malipati and Kruger/Pesvi.

Regarding agricultural areas, the supervised classification achieves an OA of 0.91 and a kappa of 0.83 in Hwange/Dete. In Gonarezhou/Malipati, the OA is 0.77 and the kappa is 0.53, while Kruger/Pesvi has an OA of 0.83 and a kappa of 0.66. Overall, the supervised classification accuracy is optimal for Hwange/Dete but more variable for Gonarezhou/Malipati and Kruger/Pesvi, where there is an equal number of confusions between the 'agricultural areas' and 'other' classes.

Finally, non-supervised classifications of landcover across the three study sites show comparable accuracy, with OA and kappa values of 0.75 and 0.67 for Hwange/Dete, 0.71 and 0.64 for Gonarezhou/Malipati, and 0.73 and 0.66 for Kruger/Pesvi. The classifications tend to overpredict the shrubland class, which is frequently confused with the mixed-woodland-shrubland and mixed-shrubland-grassland classes. In Hwange/Dete, there is also some confusion between the mixed-woodland-shrubland and woodland classes, though this is less pronounced. Overall, the woodland, mixed-shrubland-grassland, and bare soil classes are well classified across all study sites.

3.2. Simulations of the buffalo and cattle mobility across the landscapes

Fig. 4 illustrates that the areas covered by simulated centroid trajectories of buffalo herds are comparable in size to those covered by observed centroid trajectories across the three WLI study sites, although perfect overlap is not achieved due to the stochastic nature of the model. Furthermore, the model successfully reproduced the order of magnitude of KDE areas for both cattle and buffalo groups across these sites (Fig.5). For observed datasets, the annual KDE area of cattle herds ranges from 2.51 km^2 to 9.25 km^2, with an average KDE area of 5.76 km^2. In simulations, this range extends from 1.25 km^2 to 13.49 km^2, with an average KDE area of 5.04 km^2. For buffalo, observed KDE areas range from 9.72 km^2 to 158.68 km^2, with an average KDE area of 66.59 km^2, while simulations yield KDE areas from 36.21 km^2 to 220.38 km^2, with an average KDE area of 95.43 km^2. The model also captured site-specific variations, predicting smaller KDE areas in the Kruger/Pesvi WLI

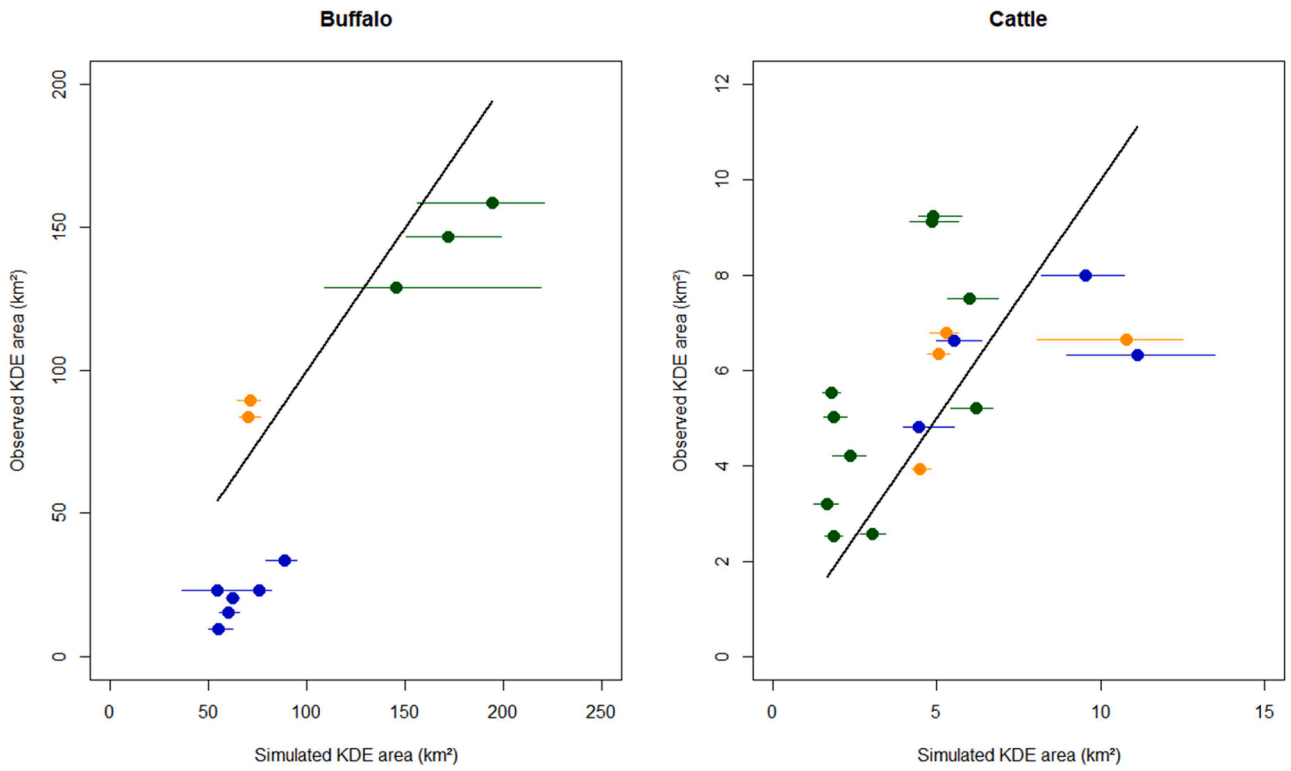

Fig. 5. Bi-dimensional representation of simulated and observed Kernel Density Estimation (KDE) of buffalo (Pearson $r = 0.90$, $p < 1.59 \times 10^{-4}$) and cattle herds (Pearson $r = 0.53$, $p = 2.45 \times 10^{-2}$) in three Wildlife-Livestock-Interfaces, Zimbabwe (diagonal line with slope = 1 and intercept = 0).

compared to the Gonarezhou/Malipati and Hwange/Dete WLI (Fig.5). It is noteworthy that site-specific variations in KDE areas are more pronounced for buffalo than for cattle (Fig.5). Finally, the model replicated variations between herds observed in the data, showing a closer fit for buffalo (Pearson $r = 0.90$, $p < 1.59 \times 10^{-4}$) compared to cattle (Pearson $r = 0.53$, $p = 2.45 \times 10^{-2}$) (Fig.5).

3.3. Simulations of buffalo - cattle contacts

In Hwange/Dete, the observed contact area was 1.18 km^2, a value situated between the simulated contact areas estimated using KDE-max (10.2 km^2) and KDE-min (7 km^2). The observed and simulated contact areas differed in both morphology and overall size: the observed KDE intersection was discontinuous and smaller, whereas the simulated KDE intersections were continuous and larger. Additionally, the observed and simulated contact areas did not overlap on the east side of the study site and only partially overlapped on the west side. The simulated contact areas were closer to the communal areas, whereas the observed contact areas were confined to the Sikumi Forest Reserve (Fig.6, Hwange/Dete). The distance between the centroids of the observed contact areas and the different simulated contact areas ranged from 1.9 to 3 km (Fig.6, Hwange/Dete).

In Gonarezhou/Malipati, the observed contact area was 1.45 km^2, while the simulated contact areas were defined by KDE-max (5.25 km^2) and KDE-min (1.1 km^2). Although the observed and simulated contact areas were within a similar surface area range, they did not perfectly overlap. The centroid distances between observed and simulated contact areas ranged from 1.3 to 2 km (Fig.6, Gonarezhou/Malipati). Like Hwange/Dete, the simulated contact areas were positioned deeper into the communal area (Fig.6, Gonarezhou/Malipati).

In Kruger/Pesvi, the observed contact area was 2.97 km^2, while the simulated contact areas defined by KDE-max and KDE-min had areas of 19.8 km^2 and 14.6 km^2, respectively. The KDE-max estimate overestimated the contact area, whereas the KDE-min estimate was quite comparable to the observed contact area (Fig.6, Kruger/Pesvi). All contact areas were located within the same general region, with similar morphology and superposition. The centroid distances between observed and simulated contact areas ranged from 0.89 to 0.9 km (Fig.6).

In Hwange/Dete, the model effectively reproduced the monthly variations in buffalo-cattle contact rates, particularly the decline in contacts from June to October, followed by an increase at the end of the hot-dry season (Fig.7a). In Gonarezhou/Malipati (Fig.7b), however, the simulated buffalo-cattle contact rates were overestimated at the end of the hot-dry season (November-December) and the beginning of the cold-dry season (April), periods during which contact rates from in-situ datasets decreased significantly. In Kruger/Pesvi (Fig.7c), the model captured the overall pattern of monthly variations in buffalo-cattle contact rates—high contact rates during the cold-dry and hot-dry seasons—although it overestimated contact rates during the rainy season (January-February).

Overall, Kruger/Pesvi exhibited the highest contact rates (annual mean = 4.19), while Hwange/Dete had the lowest (annual mean = 1.17), with Gonarezhou/Malipati showing intermediate values (annual mean = 2.65). These trends were generally well replicated by the model, with a correlation coefficient of $r = 0.53$ ($p < 10^{-3}$) (Fig.7d).

4. Discussion

4.1. Ecological implications

The model demonstrated the capacity to reproduce seasonal patterns of contact between buffalo and cattle in three different WLIs by considering only two environmental variables: surface water and land-cover, alongside the indirect consequences of herders' decisions. Using a set of simple rules that combine basic daily resource requirements (i.e., water and grazing) and herding practices (i.e., avoidance of growing crop fields), the model simulated the movements of buffalo and cattle,

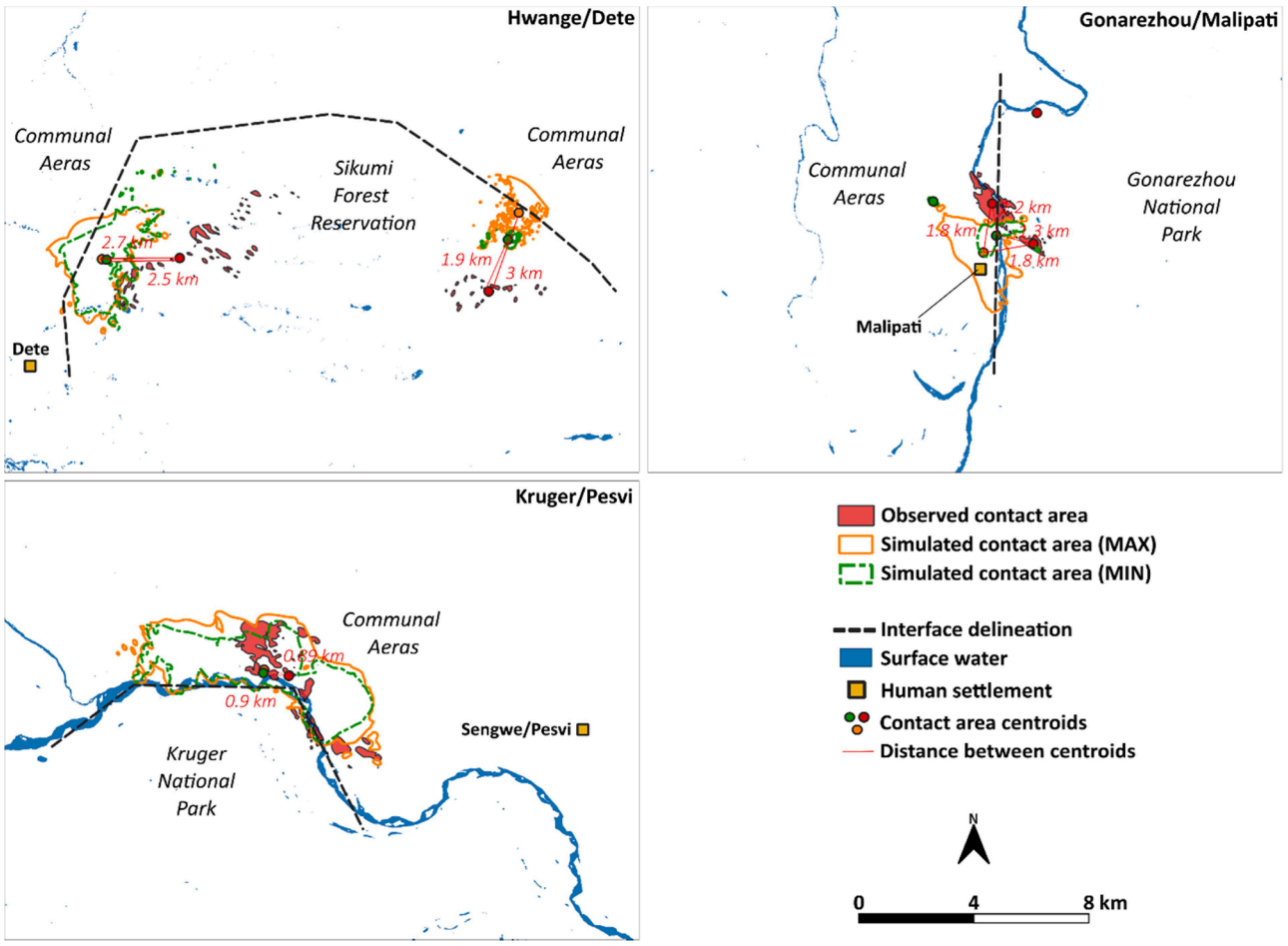

Fig. 6. Maps representing the observed and simulated contact area spatial extensions regarding the proximity of the communal area for the three study sites. Note that the interface delineations are not based on administrative borders. Their shapes and locations serve as illustration purposes and translate ecological assessments realized in-situ.

delineating areas of inter-species overlap (Fig. 4) as well as monthly variations in contact rates (Fig. 7). Within the three study sites with contrasting landscapes, the distribution of available surface water spatially concentrates animal movements around water sources and creates spatial interfaces that align with the landscape structure (Rumiano et al., 2021). Additionally, the model's consideration of grazing behaviors adds an ecological component that refines the movements of buffalo and cattle in response to landcover variability and seasonal changes. Sensitivity analysis revealed that the noise parameter is the most sensitive of all the parameters, underscoring the model's robustness to minor perturbations in structured interactions (i.e., alignment and cohesion) and its sensitivity to random fluctuations (Appendix D). The noise parameter, which introduces randomness, enables the model to capture the variability and unpredictability observed in the ecological context of the three WLIs, beyond the mapped landcover and surface water. The influence of deterministic factors such as alignment and cohesion is mitigated by stochastic phenomena not explicitly defined but implicitly suggested in our model (e.g., sudden changes in direction due to fear of predation). Consequently, the model is less deterministic despite having a set of fixed parameters (Table 1). This model design allows us to mitigate potential biases when deriving parameters that define buffalo and cattle behaviors (refer to the "Method" section and Table 1).

Despite the coherent design and outputs of the model, there are discrepancies between the model's predictions and the observed behaviors of both buffalo and cattle (Fig. 6 and Fig. 7). Specifically, the model's predictive accuracy is less reliable for cattle movements, as indicated by the lower significance of the model's outputs compared to the observed data (Fig. 5). These discrepancies may be attributed to several factors, including the limited amount of telemetry data (e.g., the bias introduced by using only two buffalo individuals to represent a herd of approximately 200, or the inherent subjectivity in classifying surface water and landcover) and the lack of external and instrumental variables relevant to buffalo and cattle ecology (e.g., herder decisions, predation). In terms of methodology, only buffalo and cattle herd centroids were used to reproduce and validate interactions between these two species. While this approach helps mitigate the issue of having a small number of collared animals as reference data, it also reduces the spatial accuracy and temporal frequency of potential contacts. This study thus contrasts with the approach used by Miguel et al. (2013), which involved individual animals to ascertain and validate contacts between buffalo and cattle at the three WLIs. Regarding external and instrumental variables influencing buffalo and cattle movements, it is noteworthy that cattle are sometimes moved further into protected areas in search of available water sources. This suggests that erratic and individual herder decisions, not accounted for by the model, may have a more significant impact than surface water availability alone. For instance, as the dry season progresses and grazing resources become depleted, cattle might move deeper into protected areas, away from the boundary. Additionally, political claims on protected land, formerly community-owned before the establishment of protected areas, could influence herder decisions and cattle movements. Using protected areas more extensively could be a tactic to exert pressure on political land claims directed towards the state (Perrotton et al., 2017). This practice may explain the observed

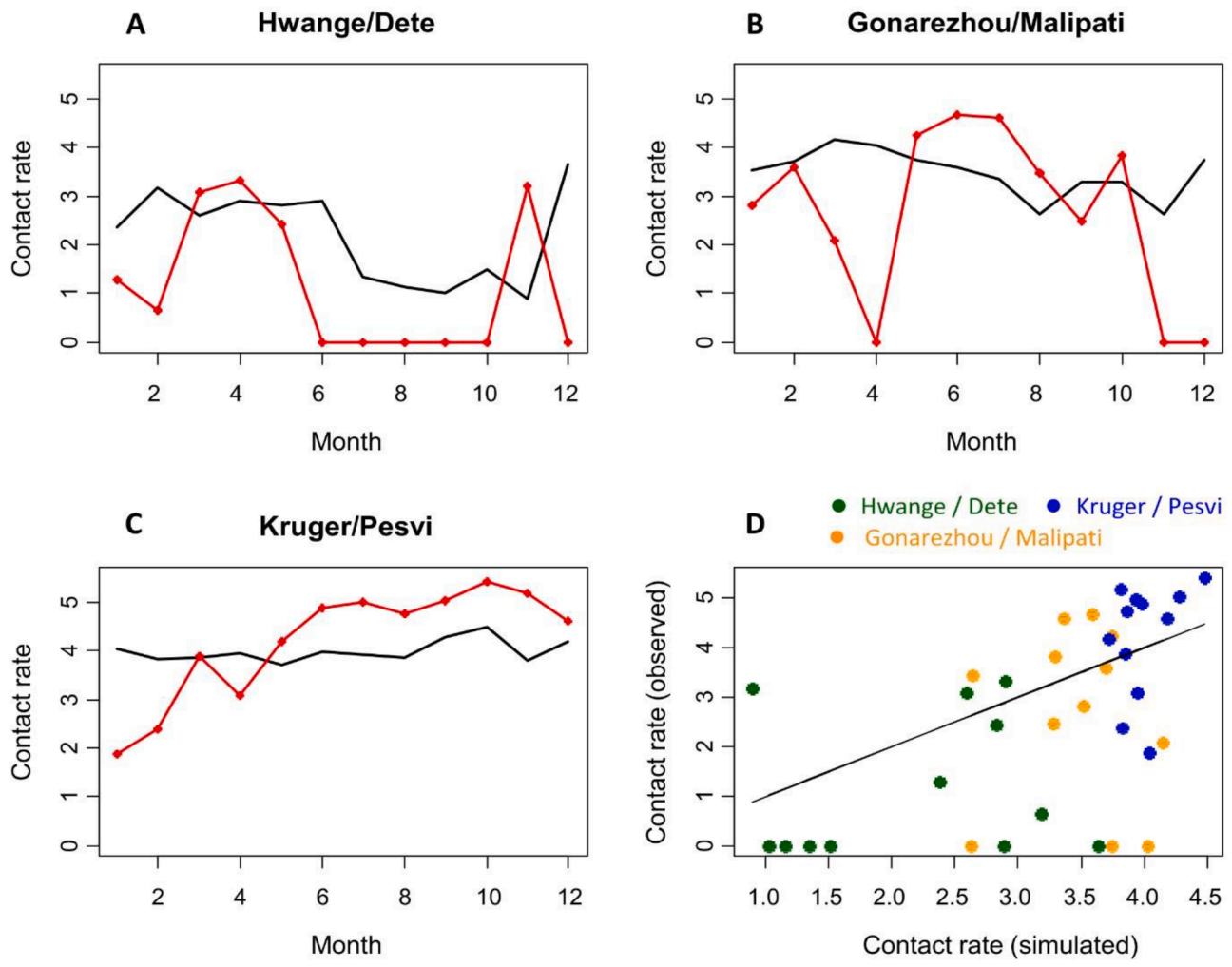

Fig. 7. Monthly variations of the buffalo-cattle contact rates computed from in-situ (red line) and simulated (black line) datasets in Hwange/Dete (A), Gonarezhou/Malipati (B) and Kruger/Pesvi (C) Wildlife-Livestock Interfaces. D) Bi-dimensional representation of simulated and observed buffalo-cattle contact rate indices in the three study sites (diagonal line with slope =1 and intercept = 0).

shift of contact areas towards the interior of the park, particularly in the Hwange/Dete study site.

Therefore, a more refined understanding of herder decision-making processes and livestock rearing practices must be integrated into the model to enhance its accuracy in reproducing cattle behaviors. Observed data for buffalo indicate that they move less towards the communal land boundary than the model predicts. This suggests that incorporating behavioral factors, such as buffalo's avoidance of cattle (Valls et al., 2018), could improve the accuracy of simulated buffalo distributions. Additionally, there are time lags between the date when environmental variables were characterized through remote sensing (i.e., 2018) and the years when in-situ telemetry data for buffalo and cattle were collected (2011–2012). Consequently, the surface water data obtained from the SRS satellite images may not align spatially and temporally with the actual surface water conditions during the telemetry data collection period. This discrepancy can introduce bias between observed and predicted movements and contacts of the focal species at the landscape scale (Fig. 7).

We also observed varying levels of accuracy in the model's spatial and temporal predictions across different study sites (Fig. 5, Fig. 6, and Fig. 7). Variations in the spatial distribution and seasonality of water sources, coupled with local topographical features, can lead to differing movement dynamics in space and time. For example, at the Hwange/Dete study site, the boundary with the protected area is not delineated by a river, unlike the other two study sites, which may directly affect the model's performance. Furthermore, local ecological conditions that are not fully or partially accounted for in the model—such as predator presence, forage availability, and human activity—could also influence its accuracy across study sites. Additionally, the Gonarezhou/Malipati and Kruger/Pesvi study sites have less telemetry data compared to the Hwange/Dete study site (Appendix A). This discrepancy in data availability can lead to variability in model accuracy, as more comprehensive and precise tracking data generally result in better model performance. Beyond differences in model accuracy across study sites, we observed variations in prediction accuracy between species, with the model struggling more to simulate cattle movements (Fig. 5). At the three WLIs, cattle movements are frequently influenced by human decisions (Perrotton et al., 2017; Valls-Fox et al., 2018a), which may not align with the natural patterns (e.g., landcover and surface water) the model is designed to simulate. Unlike buffalo, which rely on natural water sources, cattle are often provided with artificial water sources (Valls-Fox et al., 2018a). These water points can be relocated or altered based on management decisions, resulting in unpredictable movement patterns that are more challenging for the model to capture. Additionally, cattle are typically grazed in more homogeneous, managed environments such as pastures (Mudzengi et al., 2020), which may lack the varied environmental cues (e.g., diverse landcover and water sources) that the model uses to predict movement. This environmental homogeneity can reduce the model's ability to distinguish between different movement motivations. Variability in cattle management practices across the three

study sites further complicates the generalization and accuracy of movement predictions.

Nevertheless, the model, in its current configuration, allows for observations that highlight the different influences of surface water availability and landcover on the frequency and intensity of contact between buffalo and cattle at the three study sites. In Hwange/Dete, the contact rate is highest during the cropping season and the wet season, when water resources are abundant (Fig. 7). Between December and May, herders drive their cattle into protected areas to avoid damage to cultivated fields (Amon et al., 2017; Miguel et al., 2017), which aligns with the trends observed in the model's output simulations for this site. In Gonarezhou/Malipati, two peaks of contact between buffalo and cattle were observed (Fig. 7). The first peak, occurring during the cropping season in April/May, represents the attraction of buffalo to forage in agricultural areas. The model did not reproduce this trend because agricultural areas were not considered a buffalo landcover preference based on observations extrapolated from the three study sites for generalizability purposes. The second peak of activity, from September to November, corresponds to the dry season. During this period, surface water availability is limited to a few pools in the Mwenezi riverbed, and the river, being closed to communal areas, leads to more frequent contacts between buffalo and cattle. Surface water seasonal variability and potential forage resources provided by agricultural areas are the primary factors driving contact between buffalo and cattle in Gonarezhou/Malipati. In Kruger/Pesvi, the model outputs follow similar patterns, with contact rates peaking in October at the end of the dry season and decreasing during the cropping season, alternating with the winter period.

4.2. Epidemiological implications

Understanding the ecological and human-induced processes that drive the frequency, intensity, and location of inter-species contacts at the WLIs through mechanistic mathematical models can enhance our ability to quantify and characterize HWC, including pathogen circulation between wild and domestic animal species within specific multi-host systems (Caron et al., 2015; Roche et al., 2012). One advantage of mechanistic mathematical models is their ability to reproduce complex ecological processes, such as movements, watering, and foraging, with minimal empirical data (Rastetter et al., 2003). These models are promising as they can guide future data collection or clarify certain traits (e.g., targeted species' habitat preferences, herding decisions) of potential host animal species in areas where in-situ data is scarce or incomplete (Doherty and Driscoll, 2018). While some models have explored the sensitivity of pathogen dynamics to dispersal and migration rates (White et al., 2018a), few studies have examined animal movements and contacts in relation to spatially explicit landscapes and pathogen transmission (Dion et al., 2011; Lane deGraaf et al., 2013; Tracey et al., 2014). Pathogen transmission models with mechanistic representations of animal movements in space and time are still scarce (Fofana and Hurford, 2017), highlighting the need to address this gap (White et al., 2018b). Our results suggest that interspecific contacts, which carry the risk of infectious contact and pathogen transmission, are clustered and influenced by the seasonality of natural resources (Guerrini et al., 2019) and herding practices at the three studied WLIs. This information presents opportunities to improve pathogen management by controlling access to key natural resources (i.e., forage and surface water) or by adapting livestock and/or wildlife management practices to reduce the frequency of buffalo-cattle contacts. However, pathogen circulation among hosts varies along a gradient from direct to indirect transmission (Altizer et al., 2003). Thus, the definition of a 'relevant contact' for pathogen transmission depends on the specific pathogen and the spatial and temporal windows that define potential infectious contacts between focal animal species (Wielgus et al., 2021). A spatially explicit movement and contact model, such as the one developed in this study, which provides high spatial and temporal resolution outputs, could address the different temporal and spatial scales relevant for various pathogen transmission assessments.

As a future direction, the mechanistic mathematical movement and contact model presented here could be utilized to develop real-time early warning systems that coordinate efforts among governments, communities, resource partners, and international networks for pathogen transmission risk assessment (e.g., FAO's Event Mobile Application (EMA-i)). Additionally, the model could serve as a tool for testing various change scenarios, such as climate change, the rarefaction of water bodies, and changes in herd practices. This spatially explicit model could also be applied to alternative scenarios involving changes in landscape, climate, and land management to assess the impact of various disease transmission risks, as demonstrated by Dion and Lambin (2012). Moreover, analyzing spatial interactions between animal species and other entities (e.g., humans, pathogens) at different spatial and temporal scales could be incorporated into a systemic and predictive approach.

4.3. Room for improvements

Mechanistic mathematical models involve significant development and implementation costs but are less dependent on the correlation between ecological processes (e.g., movements, contacts, watering) and environmental properties (e.g., surface water, forage) compared to empirical models (Gaucherel, 2018). The ability of such mechanistic models to integrate interactions between animal behavior and related environmental variables enhances their capacity to describe holistic ecological functioning (Kearney and Porter, 2009), particularly in areas where in-situ data are lacking or expensive to collect, or when knowledge about focal animal behavior is limited. Despite the potential for generalizability demonstrated by this study, mechanistic mathematical models are often based on quantitative assessments in their design, which can lead to output redundancy and similarity (Eriksson et al., 2010). Intra-herd dynamics are simplified to parameters defining herd cohesion (see "A Spatialized Movement Model" section), while more complex field dynamics, such as the fusion-fission dynamics of buffalo herds (Caron et al., 2023b; Wielgus et al., 2020b) or cattle herding decisions influenced by collective social determinants (Valls-Fox et al., 2018a), are not fully captured. Additionally, the current temporal structure of the model, which is divided into several behavioral phases (Fig. 3), remains simplistic and relies solely on empirical knowledge and bibliographical analyses. Further information on herd practices or additional telemetry data from other areas would be valuable for testing the robustness and generalizability of the model. In its current design, the model demonstrates true generalizability potential. It is context-independent, as only input files (e.g., starting point locations, surface water, and landcover rasters) dynamically define environmental variables that dictate buffalo and cattle movements. Several functions are already implemented to read and apply potential site-specific parameters and data. The model also offers validation possibilities across study sites, ensuring its performance can be assessed in different ecological contexts. Finally, the model is capable of incorporating diverse data types, which helps capture varying environmental conditions, animal behaviors, and potential human management practices if needed.

Currently, the model does not facilitate the extrapolation of qualitative analyses, such as the propensity of buffalo to avoid contact with livestock (Miguel et al., 2013). Variables such as anthropogenic and climate changes, predator/prey dynamics, and species population heterogeneity could be considered and integrated, as they play a crucial role in influencing buffalo and cattle movements in space and time (Naidoo et al., 2012). However, the developed model has the advantage of being easily scalable and requiring only a limited amount of input data to produce coherent and meaningful results. The model is designed to efficiently handle large datasets and can utilize various data structures (e.g., rasters, shapefiles, CSV files). It supports parallel processing,

allowing for multiple simulations to be run simultaneously. To ensure and enhance the model's reproducibility, it is crucial to broadly disseminate the model's instructions, data, and code via a public online repository. Encouraging collaboration through communication and conducting workshops or webinars to train new users on the use and extension of the model would also be highly beneficial.

The democratization of remote sensing (SRS) technologies for ecologists (Remelgado et al., 2018), coupled with advances in technologies that remotely monitor animal physiology and movements (Kays and Crofoot, 2015), presents opportunities to further enhance mechanistic mathematical models such as the one developed in this study. The model's outputs and its application under different scenarios (e.g., varying climate patterns, different rearing practices) could be utilized through action research to co-produce knowledge and explore management options with local stakeholders (e.g., livestock owners, traditional authorities) to promote better coexistence between wild and domestic animals at these WLIs areas (Perrotton et al., 2017). Integrating animal movements and contacts at the landscape scale into spatially explicit epidemiological models could offer a valuable approach to address the increasing risk of pathogen transmission at the WLIs (Caron et al., 2023a).

CRediT authorship contribution statement

Florent Rumiano: Writing – review & editing, Writing – original draft, Visualization, Validation, Software, Methodology, Investigation, Formal analysis, Data curation, Conceptualization. **Eve Miguel:** Writing – review & editing, Validation, Supervision, Methodology, Investigation, Funding acquisition, Conceptualization. **Victor Dufleit:** Methodology, Investigation, Formal analysis. **Pascal Degenne:** Writing – review & editing, Supervision, Software, Methodology, Formal analysis, Conceptualization. **Cédric Gaucherel:** Writing – review & editing, Methodology, Investigation, Conceptualization. **Hugo Valls-Fox:** Writing – review & editing, Investigation. **Michel de Garine-Wichatitsky:** Writing – review & editing, Validation, Supervision, Conceptualization. **Edson Gandiwa:** Writing – review & editing. **Alexandre Caron:** Writing – review & editing, Validation, Supervision, Methodology, Investigation, Conceptualization. **Annelise Tran:** Writing – review & editing, Visualization, Validation, Supervision, Resources, Methodology, Investigation, Funding acquisition, Formal analysis, Data curation, Conceptualization.

Declaration of competing interest

The authors declare that they have no known competing financial interests or personal relationships that could have appeared to influence the work reported in this paper.

Data availability

The data used in this article are provided in the "data availability" section and cab be downloaded via DOI links

Acknowledgments

This work is part of a thesis integrated into the TEMPO (TElédétection et Modélisation sPatiale de la mObilité animale) - https://tempo.cirad.fr/en and is implemented under the framework of the Research Platform "Production and Conservation in Partnership" - https://www.rp-pcp.org/. The PhD thesis has been funded by I-SITE MUSE (Montpellier Unversité d'Excellence) —https://muse.edu.umontpellier.fr/en/muse-isite/ through the French National Research Agency (ANR) under the "Investissements d'avenir" program, grant number ANR-16-IDEX-0006.

Several other projects need to be acknowledged in regard to the telemetry data availability: the European Union with the EU-PARSEL project, the Zimbabwean office of the Food and Agriculture Organisation (FAO), the project, SAVARID, the AHEAD initiative, the French ANR (FEAR project ANR-08-BLAN-0022) and the FSP-RenCaRe project.

Data availability

The Sentinel-2 images are freely available at https://scihub.copernicus.eu/dhus/#/home after login.

The landcover maps are available to download at CIRAD depository website:

Rumiano, Florent; Miguel, Eve; Caron, Alexandre; Dupuy, Stephane; Tran, Annelise, 2022, "Land cover map, Malipati site, Gonarezhou National Park, Zimbabwe", https://doi.org/10.18167/DVN1/2SFOA5, CIRAD Dataverse, V1

Rumiano, Florent; Miguel, Eve; Caron, Alexandre; Dupuy, Stéphane; Tran, Annelise, 2022, "Land cover map, Pesvi site, Kruger National Park, Zimbabwe", https://doi.org/10.18167/DVN1/ZLIQIL, CIRAD Dataverse, V1

Rumiano, Florent; Miguel, Eve; Valls-Fox, Hugo; Chamaillé-Jammes, Simon; Caron, Alexandre; Tran, Annelise, 2020, "Land cover map, Dete site, Hwangue National Park, Zimbabwe", https://doi.org/10.18167/DVN1/BJJZJV, CIRAD Dataverse, V1

The surface water map is available to download at CIRAD depository website:

Rumiano, Florent; Miguel, Eve; Caron, Alexandre; Dupuy, Stéphane; Tran, Annelise, 2022, "Monthly surface water maps, Gonarezhou National Park, Zimbabwe, 2018", https://doi.org/10.18167/DVN1/O9COVW, CIRAD Dataverse, V1

Rumiano, Florent; Miguel, Eve; Caron, Alexandre; Dupuy, Stéphane; Tran, Annelise, 2022, "Monthly surface water maps, North Kruger National Park, 2018", https://doi.org/10.18167/DVN1/DAVZUY, CIRAD Dataverse, V1

Rumiano, Florent; Miguel, Eve; Valls-Fox, Hugo; Chamaillé-Jammes, Simon; Caron, Alexandre; Tran, Annelise, 2020, "Monthly surface water maps, Hwange National Park, Zimbabwe, 2018", https://doi.org/10.18167/DVN1/KPSYME, CIRAD Dataverse, V1

The buffalo and cattle GPS data access are subject to authors' authorization.

The buffalo and cattle movement scripts, a sample of the necessary model input data (i.e., surface water, landcover, simulation starting location) and a step-by-step guide to use the models in the Ocelet platform are available to download at CIRAD depository website:

Rumiano, Florent; Tran, Annelise; Degenne, Pascal; Dufleit, Victor; Caron, Alexandre; Miguel, Eve, 2023, "Spatial models of animal mobility: buffalo and cattle in Southern Africa", https://doi.org/10.18167/DVN1/T8DX7U, CIRAD Dataverse, V2

Supplementary materials

Supplementary material associated with this article can be found, in the online version, at doi:10.1016/j.ecolmodel.2024.110863.

References

Altizer, S., Harvell, D., Friedle, E., 2003. Rapid evolutionary dynamics and disease threats to biodiversity. Trends Ecol. Evol. (Amst.) 18 (11), 589–596. https://doi.org/10.1016/J.TREE.2003.08.013.

Arraut, E.M., Loveridge, A.J., Chamaillé-Jammes, S., Valls-Fox, H., Macdonald, D.W., 2018. The 2013-2014 vegetation structure map of Hwange National Park, Zimbabwe, produced using free satellite images and software. Koedoe 60 (1), 1–10. https://doi.org/10.4102/KOEDOE.V60I1.1497.

Bellón, B., Bégué, A., Seen, D., lo, de Almeida, C.A., Simões, M., 2017. A remote sensing approach for regional-scale mapping of agricultural land-use systems based on NDVI time series. Remote Sens. 2017 9 (6), 600. https://doi.org/10.3390/RS9060600. Vol. 9, Page 600.

Benhamou, S., 2014. Of scales and stationarity in animal movements. Ecol. Lett. 17 (3), 261–272. https://doi.org/10.1111/ELE.12225.

Börger, L., Franconi, N., De Michele, G., Gantz, A., Meschi, F., Manica, A., Lovari, S., Coulson, T.I.M., 2006. Effects of sampling regime on the mean and variance of home range size estimates. J. Anim. Ecol. 75 (6), 1393–1405. https://doi.org/10.1111/j.1365-2656.2006.01164.x.

Burrough, P.A., van Gaans, P.F.M., MacMillan, R.A., 2000. High-resolution landform classification using fuzzy k-means. Fuzzy. Sets. Syst. 113 (1), 37–52. https://doi.org/10.1016/S0165-0114(99)00011-1.

Caron, A., Angel Barasona, J., Miguel, E., Michaux, J., de Garine-Wichatitsky, M., 2021. Characterisation of Wildlife-Livestock Interfaces: the Need for Interdisciplinary Approaches and a Dedicated Thematic Field. 339–367. https://doi.org/10.1007/978-3-030-65365-1_11.

Caron, A., Bennitt, E., Wielgus, E., Cornelis, D., Miguel, E., de Garine-Wichatitsky, M., 2023b. African Buffalo Social Dynamics: what Is a Buffalo Herd? Ecol. Manag. Afric. Buffalo 153–179. https://doi.org/10.1017/9781009006828.010.

Caron, A., Cappelle, J., Cumming, G.S., de Garine-Wichatitsky, M., Gaidet, N., 2015. Bridge hosts, a missing link for disease ecology in multi-host systems. Vet. Res. 46 (1), 1–11. https://doi.org/10.1186/S13567-015-0217-9/TABLES/2.

Caron, A., Miguel, E., Gomo, C., Makaya, P., Pfukenyi, D.M., Foggin, C., Hove, T., de Garine-Wichatitsky, M., 2013. Relationship between burden of infection in ungulate populations and wildlife/livestock interfaces. Epidemiol. Infect. 141 (7), 1522–1535. https://doi.org/10.1017/S0950268813000204.

Caron, A., Rumiano, F., Wielgus, E., Miguel, E., Tran, A., Bah, M.T., Grosbois, V., de Garine-Wichatitsky, M., 2023a. Characterization of buffalo/cattle interactions for assessing pathogen transmission. Ecol. Manag. Afric. Buffalo 269–293. https://doi.org/10.1017/9781009006828.015.

Carter, N.H., Baeza, A., Magliocca, N.R., 2020. Emergent conservation outcomes of shared risk perception in human-wildlife systems. Conservat. Biol. 34 (4), 903–914. https://doi.org/10.1111/COBI.13473.

Chagumaira, C., Rurinda, J., Nezomba, H., Mtambanengwe, F., Mapfumo, P., 2016. Use patterns of natural resources supporting livelihoods of smallholder communities and implications for climate change adaptation in Zimbabwe. Environ. Dev. Sustain. 18 (1), 237–255. https://doi.org/10.1007/S10668-015-9637-Y/FIGURES/5.

Chamaillé-Jammes, S., Fritz, H., Madzikanda, H., 2009. Piosphere contribution to landscape heterogeneity: a case study of remote-sensed woody cover in a high elephant density landscape. Ecography 32 (5), 871–880. https://doi.org/10.1111/J.1600-0587.2009.05785.X.

Chamaillé-Jammes, S., Valeix, M., Fritz, H., 2007. Managing heterogeneity in elephant distribution: interactions between elephant population density and surface-water availability. J. Appl. Ecol. 44 (3), 625–633. https://doi.org/10.1111/J.1365-2664.2007.01300.X.

Chigonda, T., 2018. More than just story telling: a review of biodiversity conservation and utilisation from precolonial to postcolonial Zimbabwe. Scientifica (Cairo) 2018. https://doi.org/10.1155/2018/6214318.

Chigwenhese, L., Murwira, A., Zengeya, F.M., Masocha, M., de Garine-Wichatitsky, M., Caron, A., 2016. Monitoring African buffalo (Syncerus caffer) and cattle (Bos taurus) movement across a damaged veterinary control fence at a Southern African wildlife/livestock interface. Afr. J. Ecol. 54 (4), 415–423. https://doi.org/10.1111/AJE.12288.

Decker, D.J., Evensen, D.T.N., Siemer, W.F., Leong, K.M., Riley, S.J., Wild, M.A., Castle, K.T., Higgins, C.L., 2010. Understanding risk perceptions to enhance communication about human-wildlife interactions and the impacts of zoonotic disease. ILAR. J. 51 (3), 255–261. https://doi.org/10.1093/ILAR.51.3.255.

Degenne, P., lo Seen, D., 2016. Ocelet: simulating processes of landscape changes using interaction graphs. SoftwareX. 5, 89–95. https://doi.org/10.1016/J.SOFTX.2016.05.002.

Dion, E., Lambin, E.F., 2012. Scenarios of transmission risk of foot-and-mouth with climatic, social and landscape changes in southern Africa. Applied Geography 35 (1–2), 32–42. https://doi.org/10.1016/J.APGEOG.2012.05.001.

Dion, E., VanSchalkwyk, L., Lambin, E.F., 2011. The landscape epidemiology of foot-and-mouth disease in South Africa: a spatially explicit multi-agent simulation. Ecol Modell 222 (13), 2059–2072. https://doi.org/10.1016/J.ECOLMODEL.2011.03.026.

Distefano, E., 2005. Human-Wildlife Conflict Worldwide: Collection of Case Studies, Analysis of Management Strategies and Good Practices. Food and Agricultural Organization of the United Nations (FAO) Sustainable Agriculture and Rural Development Initiative (SARDI). https://doi.org/10.4060/CC7285EN.

Doherty, T.S., Driscoll, D.A., 2018. Coupling movement and landscape ecology for animal conservation in production landscapes. Proc. R. Soc. B: Biol. Sci. 285 (1870). https://doi.org/10.1098/RSPB.2017.2272.

Drusch, M., del Bello, U., Carlier, S., Colin, O., Fernandez, V., Gascon, F., Hoersch, B., Isola, C., Laberinti, P., Martimort, P., Meygret, A., Spoto, F., Sy, O., Marchese, F., Bargellini, P., 2012. Sentinel-2: eSA's optical high-resolution mission for GMES operational services. Remote Sens. Environ. 120, 25–36. https://doi.org/10.1016/J.RSE.2011.11.026.

Du, Y., Zhang, Y., Ling, F., Wang, Q., Li, W., Li, X., 2016. Water Bodies' mapping from sentinel-2 imagery with modified normalized difference water index at 10-m spatial resolution produced by sharpening the SWIR band. Remote Sens. 2016 8 (4), 354. https://doi.org/10.3390/RS8040354. Vol. 8, Page 354.

Duong, T. (2021). ks: kernel Smoothing. R package version 1.13.3. https://CRAN.R-project.org/package=ks.

Eklund, A., López-Bao, J.V., Tourani, M., Chapron, G., Frank, J., 2017. Limited evidence on the effectiveness of interventions to reduce livestock predation by large carnivores. Sci. Rep. 7 (1). https://doi.org/10.1038/S41598-017-02323-W.

Eriksson, A., Nilsson Jacobi, M., Nyström, J., Tunstrøm, K., 2010. Determining interaction rules in animal swarms. Behav. Ecol. 21 (5), 1106–1111. https://doi.org/10.1093/BEHECO/ARQ118.

Ferguson, K., Hanks, J., 2012. The effects of protected area and veterinary fencing on wildlife conservation in Southern. Africa. Parks 18.1 (no 1), 49–60. https://parksjournal.com/wp-content/uploads/2012/09/PARKS-18.1-Ferguson-10.2305IUCN.CH_.2012.PARKS-18-1.KF_.en_.pdf.

Fern, R.R., Foxley, E.A., Bruno, A., Morrison, M.L., 2018. Suitability of NDVI and OSAVI as estimators of green biomass and coverage in a semi-arid rangeland. Ecol. Indic. 94, 16–21. https://doi.org/10.1016/J.ECOLIND.2018.06.029.

Fofana, A.M., Hurford, A., John', S., Labrador, C., 2017. Mechanistic movement models to understand epidemic spread. Philos. Trans. R. Soc. B: Biol. Sci. 372 (1719). https://doi.org/10.1098/RSTB.2016.0086.

Frank, B., Glikman, J.A., Marchini, S., 2019. Human-wildlife interactions: turning conflict into coexistence. Human-Wildlife Interactions: turning Conflict into Coexistence, 1–464. https://doi.org/10.1017/9781108235730.

Fynn, R.W.S., Augustine, D.J., Peel, M.J.S., de Garine-Wichatitsky, M., 2016. Strategic management of livestock to improve biodiversity conservation in African savannahs: a conceptual basis for wildlife–livestock coexistence. J. Appl. Ecol. 53 (2), 388–397. https://doi.org/10.1111/1365-2664.12591.

Fynn, R.W.S., Bonyongo, M.C., 2011. Functional conservation areas and the future of Africa's wildlife. Afr. J. Ecol. 49 (2), 175–188. https://doi.org/10.1111/J.1365-2028.2010.01245.X.

Gaucherel, C., 2011. Wavelet analysis to detect regime shifts in animal movement. Comput. Ecol. Softw. 1 (2), 69–85. https://doaj.org/article/b2351eb266c24ee4a1ac05608d238000.

Gaucherel, C., 2018. Physical concepts and ecosystem ecology: a revival? J. Ecosyst. Ecogr. 8 (259). https://doi.org/10.4172/2157-7625.1000259.

Giuggioli, L., Kenkre, V.M., 2014. Consequences of animal interactions on their dynamics: emergence of home ranges and territoriality. Mov. Ecol. 2, 20. https://doi.org/10.1186/s40462-014-0020-7.

Grégoire, G., Chaté, H., Tu, Y., 2003. Moving and staying together without a leader. Physica D: Nonlinear Phenomena 181 (3–4), 157–170. https://doi.org/10.1016/S0167-2789(03)00102-7.

Grimm, Volker, Railsback, Steven F., 2005. Individual-based Modeling and Ecology. Princeton University Press, Princeton. https://doi.org/10.1515/9781400850624.

Gross, E.M., Lahkar, B.P., Subedi, N., Nyirenda, V.R., Lichtenfeld, L.L., Jakoby, O., 2018. Seasonality, crop type and crop phenology influence crop damage by wildlife herbivores in Africa and Asia. Biodivers. Conserv. 27 (8), 2029–2050. https://doi.org/10.1007/S10531-018-1523-0/TABLES/2.

Guerbois, C., Chapanda, E., Fritz, H., 2012. Combining multi-scale socio-ecological approaches to understand the susceptibility of subsistence farmers to elephant crop raiding on the edge of a protected area. J. Appl. Ecol. 49 (5), 1149–1158. https://doi.org/10.1111/J.1365-2664.2012.02192.X.

Guerrini, L., Pfukenyi, D.M., Etter, E., Bouyer, J., Njagu, C., Ndhlovu, F., Bourgarel, M., de Garine-Wichatitsky, M., Foggin, C., Grosbois, V., Caron, A., 2019. Spatial and seasonal patterns of FMD primary outbreaks in cattle in Zimbabwe between 1931 and 2016. Vet. Res. 50 (1), 1–12. https://doi.org/10.1186/S13567-019-0690-7/TABLES/4.

Hansen, A.J., DeFries, R., 2007. Land use change around nature reserves: implications for sustaining biodiversity. Ecological Applications: A Publication of the Ecological Society of America 17 (4), 972–973. https://doi.org/10.1890/05-1112.

IPCC, 2023. Climate Change 2023: synthesis Report. In: Lee, H., Romero, J. (Eds.), Climate Change 2023: synthesis Report. Contribution of Working Groups I, II and III to the Sixth Assessment Report of the Intergovernmental Panel On Climate Change Core Writing Team 35–115. https://doi.org/10.59327/IPCC/AR6-9789291691647.

Jonsen, I.D., Flemming, J.M., Myers, R.A., 2005. Robust state-space modeling of animal movement data. Ecology 86, 2874–2880. https://doi.org/10.1890/04-1852.

Kays, R., Crofoot, M.C., Jetz, W., Wikelski, M., 2015. Terrestrial animal tracking as an eye on life and planet. Science 348 (6240). https://doi.org/10.1126/SCIENCE.AAA2478/SUPPL_FILE/KAYS.SM.PDF aaa2478.

Kearney, M., Porter, W., 2009. Mechanistic niche modelling: combining physiological and spatial data to predict species' ranges. Ecol. Lett. 12 (4), 334–350. https://doi.org/10.1111/J.1461-0248.2008.01277.X.

Kock, R.A., Bengis, R.G., Shiferaw, F.D., Gakuya, F., Mdetele, D., Prins, H.H.T., Caron, A., Kock, M.D., 2023. African buffalo and colonial cattle: is 'Systems Change' the best future for farming and nature in Africa? Ecol. Manag. Afric. Buffalo 320–350. https://doi.org/10.1017/9781009006828.017.

König, H.J., Kiffner, C., Kramer-Schadt, S., Fürst, C., Keuling, O., Ford, A.T., 2020. Human-wildlife coexistence in a changing world. Conservat. Biol.: J. Soc. Conservat. Biol. 34 (4), 786–794. https://doi.org/10.1111/COBI.13513.

Lane deGraaf, K.E., Kennedy, R.C., Arifin, S.M.N., Madey, G.R., Fuentes, A., Hollocher, H., 2013. A test of agent-based models as a tool for predicting patterns of pathogen transmission in complex landscapes. BMC Ecol. 13 (1), 1–12. https://doi.org/10.1186/1472-6785-13-35/TABLES/3.

Laver, P.N., Kelly, M.J., 2008. A critical review of home range studies. J. Wildlife Manag. 72 (1), 290–298. https://doi.org/10.2193/2005-589.

Madden, F., 2004. Creating coexistence between humans and wildlife: global perspectives on local efforts to address human–wildlife conflict. Human Dimension. Wildlife 9 (4), 247–257. https://doi.org/10.1080/10871200490505675.

Mbise, F.P., 2021. Attacks on humans and retaliatory killing of wild carnivores in the eastern Serengeti Ecosystem, Tanzania. J. Ecol. Natural Environ. 13 (4), 110–116. https://doi.org/10.5897/JENE2021.0908.

Mercier, A., Betbeder, J., Rumiano, F., Baudry, J., Gond, V., Blanc, L., Bourgoin, C., Cornu, G., Ciudad, C., Marchamalo, M., Poccard-Chapuis, R., Hubert-Moy, L., 2019. Evaluation of Sentinel-1 and 2 time series for land cover classification of forest–agriculture mosaics in temperate and tropical landscapes. Remote Sens. 2019 11 (8), 979. https://doi.org/10.3390/RS11080979. Vol. 11, Page 979.

Miguel, E., 2012. Contacts et diffusion de pathogènes des ongulés sauvages aux ongulés domestiques africains. Thèse de Doctorat : Parasitologie, Microbiologie : Université Montpellier 2 (UM2) 2 vol. https://www.theses.fr/2012MON20064.

Miguel, E., Grosbois, V., Caron, A., Boulinier, T., Fritz, H., Cornelis, D., Foggin, C., Makaya, P.v., Tshabalala, P.T., de Garine-Wichatitsky, M., 2013. Contacts and foot and mouth disease transmission from wild to domestic bovines in Africa. Ecosphere, 4 (4), 1–32. https://doi.org/10.1890/ES12-00239.1.

Miguel, E., Grosbois, V., Fritz, H., Caron, A., de Garine-Wichatitsky, M., Nicod, F., Loveridge, A.J., Stapelkamp, B., Macdonald, D.W., Valeix, M., 2017. Drivers of foot-and-mouth disease in cattle at wild/domestic interface: insights from farmers, buffalo and lions. Divers. Distribut. 23 (9), 1018–1030. https://doi.org/10.1111/DDI.12585.

Morales, J.M., Haydon, D.T., Frair, J., Holsinger, K.E., Fryxell, J.M., 2004. Extracting more out of relocation data: building movement models as mixtures of random walks. Ecology 85, 2436–2445. https://doi.org/10.1890/03-0269.

Mudzengi, C.P., Murwira, A., Zengeya, F.M., Halimani, T., Fritz, H., Murungweni, C., 2020. Mapping key browse resources in a heterogeneous agricultural landscape. Afr. J. Range Forage Sci. 37 (2), 181–189. https://doi.org/10.2989/10220119.2020.1740892.

Murwira, Amon, de Garine-Wichatitsky, M., Zengeya, F., Poshiwa, X., Matema, S., Caron, A., Guerbois, C., Hellard, E., Fritz, H., 2017. Resource gradients and movements across the edge of transfrontier parks. Transfrontier Conservat. Areas 123–136. https://doi.org/10.4324/9781315147376-7.

Mutanga, C.N., Muboko, N., Gandiwa, E., 2017. Protected area staff and local community viewpoints: a qualitative assessment of conservation relationships in Zimbabwe. PLoS ONE 12 (5), e0177153. https://doi.org/10.1371/JOURNAL.PONE.0177153.

Naidoo, R., du Preez, P., Stuart-Hill, G., Chris Weaver, L., Jago, M., Wegmann, M., 2012. Factors affecting intraspecific variation in home range size of a large African herbivore. Landsc. Ecol. 27 (10), 1523–1534. https://doi.org/10.1007/S10980-012-9807-3/FIGURES/2</bib.

Odadi, W.O., Karachi, M.K., Abdulrazak, S.A., Young, T.P., 2011. African wild ungulates compete with or facilitate cattle depending on season. Science 333 (6050), 1753–1755. https://doi.org/10.1126/SCIENCE.1208468/SUPPL_FILE/ODADI-SOM.REVISION.1.PDF</bib.

Ogutu, J.O., Reid, R.S., Piepho, H.P., Hobbs, N.T., Rainy, M.E., Kruska, R.L., Worden, J. S., Nyabenge, M., 2014. Large herbivore responses to surface water and land use in an East African savanna: implications for conservation and human-wildlife conflicts. Biodivers. Conserv. 23 (3), 573–596. https://doi.org/10.1007/S10531-013-0617-Y/FIGURES/6</bib.

Owen-Smith, N., Fryxell, J.M., Merrill, E.H., 2010. Foraging theory upscaled: the behavioural ecology of herbivore movement. Philos. Trans. R. Soc. B: Biol. Sci. 365 (1550), 2267–2278. https://doi.org/10.1098/RSTB.2010.0095.

Perrotton, A., de Garine-Wichatitsky, M., Valls-Fox, H., Lepage, C., 2017. My cattle and your park: codesigning a role-playing game with rural communities to promote multistakeholder dialogue at the edge of protected areas. Ecol. Soc. 22 (1). https://doi.org/10.5751/ES-08962-220135. Published Online: Mar 06, 2017 |.

Rastetter, E.B., Aber, J.D., Peters, D.P.C., Ojima, D.S., Burke, I.C., 2003. Using Mechanistic Models to Scale Ecological Processes across Space and Time. Bioscience 53 (1), 68–76. https://doi.org/10.1641/0006-3568(2003)053[0068:UMMTSE]2.0.CO;2.

Remelgado, R., Leutner, B., Safi, K., Sonnenschein, R., Kuebert, C., Wegmann, M., 2018. Linking animal movement and remote sensing – mapping resource suitability from a remote sensing perspective. Remote Sens. Ecol. Conserv. 4 (3), 211–224. https://doi.org/10.1002/RSE2.70.

Roche, B., Dobson, A.P., Guégan, J.F., Rohani, P., 2012. Linking community and disease ecology: the impact of biodiversity on pathogen transmission. Philos. Trans. R. Soc. B: Biol. Sci. 367 (1604), 2807. https://doi.org/10.1098/RSTB.2011.0364.

Rumiano, F., Gaucherel, C., Degenne, P., Miguel, E., Chamaillé-Jammes, S., Valls-Fox, H., Cornélis, D., de Garine-Wichatitsky, M., Fritz, H., Caron, A., Tran, A., 2021. Combined use of remote sensing and spatial modelling: when surface water impacts buffalo (Syncerus Caffer Caffer) movements in savanna environments. The International Archives of the Photogrammetry. Remote Sens. Spatial Inf. Sci. 631–638. https://doi.org/10.5194/ISPRS-ARCHIVES-XLIII-B3-2021-631-2021. XLIII-B3-2021(B3-2021.

Rumiano, F., Wielgus, E., Miguel, E., Chamaillé-Jammes, S., Valls-Fox, H., Cornélis, D., de Garine-Wichatitsky, M., Fritz, H., Caron, A., Tran, A., 2020. Remote sensing of environmental drivers influencing the movement ecology of sympatric wild and domestic ungulates in semi-arid savannas, a review. Remote Sens. 2020 12 (19), 3218. https://doi.org/10.3390/RS12193218. Vol. 12, Page 3218.

Sawyer, H., Kauffman, M.J., Middleton, A.D., Morrison, T.A., Nielson, R.M., Wyckoff, T. B., 2013. A framework for understanding semi-permeable barrier effects on migratory ungulates. J. Appl. Ecol. 50, 68–78. https://doi.org/10.1111/1365-2664.12013.

Schuster, C., Förster, M., Kleinschmit, B., 2012. Testing the red edge channel for improving land-use classifications based on high-resolution multi-spectral satellite data. Int. J. Remote Sens. 33 (17), 5583–5599. https://doi.org/10.1080/01431161.2012.666812.

Shrader, A.M., Kotler, B.P., Brown, J.S., Kerley, G.I.H., 2008. Providing water for goats in arid landscapes: effects on feeding effort with regard to time period, herd size and secondary compounds. Oikos. 117 (3), 466–472. https://doi.org/10.1111/J.2007.0030-1299.16410.X.

Silverman, B.W., 1998. Density Estimation for Statistics and Data Analysis, 1st ed. Routledge. https://doi.org/10.1201/9781315140919.

Sumpter, D.J.T., 2006. The principles of collective animal behaviour. Phil. Trans. R. Soc., B 361, 5–22. https://doi.org/10.1098/rstb.2005.1733.

Tracey, J.A., Bevins, S.N., Vandewoude, S., Crooks, K.R., 2014. An agent-based movement model to assess the impact of landscape fragmentation on disease transmission. Ecosphere 5 (9), 1–24. https://doi.org/10.1890/ES13-00376.1.

Treves, A., Wallace, R.B., Naughton-Treves, L., Morales, A., 2006. Co-Managing Human–Wildlife Conflicts: A Review, 11. Human Dimensions of Wildlife, pp. 383–396. https://doi.org/10.1080/10871200600984265.

Valls-Fox, H., Chamaillé-Jammes, S., de Garine-Wichatitsky, M., Perrotton, A., Courbin, N., Miguel, E., Guerbois, C., Caron, A., Loveridge, A., Stapelkamp, B., Muzamba, M., Fritz, H., 2018a. Water and cattle shape habitat selection by wild herbivores at the edge of a protected area. Anim. Conserv. 21 (5), 365–375. https://doi.org/10.1111/ACV.12403.

Valls-Fox, H., de Garine-Wichatitsky, M., Fritz, H., Chamaillé-Jammes, S., 2018b. Resource depletion versus landscape complementation: habitat selection by a multiple central place forager. Landsc. Ecol. 33 (1), 127–140. https://doi.org/10.1007/S10980-017-0588-6/FIGURES/5.

Wang, G., Hobbs, N.T., Boone, R.B., Illius, A.W., Gordon, I.J., Gross, J.E., Hamlin, K.L., 2006. Spatial and temporal variability modify density dependence in populations of large herbivores. Ecology 87 (1), 95–102. https://doi.org/10.1890/05-0355.

Warchol, G.L., Zupan, L.L., Clack, W., 2003. Transnational Criminality: an Analysis of the Illegal Wildlife Market in Southern Africa. Int. Crim. Justice Rev. 13 (1), 1–27. https://doi.org/10.1177/105756770301300101</bib.

Westley, P.A.H., Berdahl, A.M., Torney, C.J., Biro, D., 2018. Collective movement in ecology: from emerging technologies to conservation and management. Philos. Trans. R. Soc. B: Biol. Sci. 373 (1746). https://doi.org/10.1098/RSTB.2017.0004.

White, L.A., Forester, J.D., Craft, M.E., 2018a. Disease outbreak thresholds emerge from interactions between movement behavior, landscape structure, and epidemiology. Proc. Natl. Acad. Sci. U.S.A. 115 (28), 7374–7379. https://doi.org/10.1073/PNAS.1801383115/SUPPL_FILE/PNAS.1801383115.SAPP.PDF.

White, L.A., Forester, J.D., Craft, M.E., 2018b. Dynamic, spatial models of parasite transmission in wildlife: their structure, applications and remaining challenges. J. Anim. Ecol. 87 (3), 559–580. https://doi.org/10.1111/1365-2656.12761.

Wielgus, E., 2020a. The Social Dynamics of the Cape buffalo and the Epidemiological Implications. The Manchester Metropolitan University. P.h.D. Thesis. https://e-space.mmu.ac.uk/627391/1/Elodie%20Wielgus%20-%20FINAL%20VERSION%20THESIS.pdf.

Wielgus, E., Caron, A., Bennitt, E., de Garine-Wichatitsky, M., Cain, B., Fritz, H., Miguel, E., Cornélis, D., Chamaillé-Jammes, S., 2021. Inter-Group Social Behavior, Contact Patterns and Risk for Pathogen Transmission in Cape Buffalo Populations. J. Wildl. Manage. 85 (8), 1574–1590. https://doi.org/10.1002/JWMG.22116.

Wielgus, E., Cornélis, D., de Garine-Wichatitsky, M., Cain, B., Fritz, H., Miguel, E., Valls-Fox, H., Caron, A., Chamaillé-Jammes, S., 2020b. Are fission–fusion dynamics consistent among populations? A large-scale study with Cape buffalo. Ecol. Evol. 10 (17), 9240–9256. https://doi.org/10.1002/ECE3.6608.

Wiens, J.A., 1989. Spatial Scaling in Ecology. Funct. Ecol. 3 (4), 385. https://doi.org/10.2307/2389612.

Wittemyer, G., Elsen, P., Bean, W.T., Burton, A.C.O., Brashares, J.S., 2008. Accelerated human population growth at protected area edges. Science 321 (5885), 123–126. https://doi.org/10.1126/SCIENCE.1158900/SUPPL_FILE/WITTEMYER.SOM.PDF.

Worton, B.J., 1989. Kernel methods for estimating the utilization distribution in home-range studies. Ecology 70 (1), 164–168. https://doi.org/10.2307/1938423.

Zhao, Y., Potgieter, A.B., Zhang, M., Wu, B., Hammer, G.L., 2020. Predicting wheat yield at the field scale by combining high-resolution sentinel-2 satellite imagery and crop modelling. Remote Sens. 2020 12 (6), 1024. https://doi.org/10.3390/RS12061024. Vol. 12, Page 1024.